Table 1. Results of right heart catheterization

RA (mmHg)	14
PA systole (mmHg)	73
PA diastole (mmHg)	26
PA mean (mmHg)	49
PCWP (mmHg)	8
Cardiac output (l/min)	3.8
Cardiac index (l/min/m^2)	2.4
PA saturation (%)	47
PVR (Wood units)	10.8

Data on first admission in February 2008. Cardiac output was obtained by thermodilution method
RA, right atrium; PA, pulmonary artery; PCWP, pulmonary capillary wedge pressure; PVR, pulmonary vascular resistance

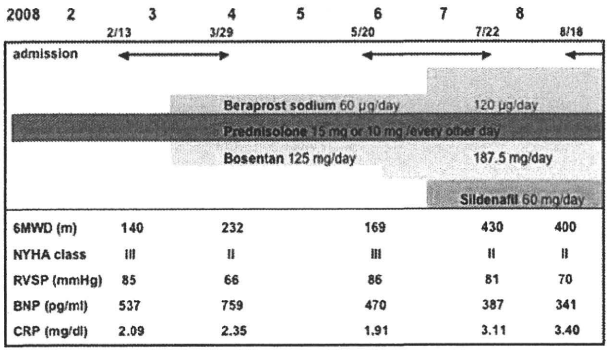

Fig. 1. Clinical course of the patient before tocilizumab treatment. *6MWD*, 6-min walking distance; *NYHA*, New York Heart Association; *RVSP*, right ventricular systolic pressure; *BNP*, brain natriuretic peptide; *CRP*, C-reactive protein

admission, her blood pressure was 110/80 mmHg and heart rate 96 beats/min, and her arterial blood gas on room air revealed a PaO_2 65.5 mmHg/$PaCO_2$ 26.6 mmHg. Chest radiography revealed pulmonary congestion and cardiomegaly, and an electrocardiogram showed right atrial enlargement and right ventricular hypertrophy. Brain natriuretic peptide (BNP) was 537 pg/ml, serum uric acid (UA) 6.5 mg/dl, and CRP 2.09 mg/dl. Six-minute walking distance (6MWD) was 140 m at that time (Fig. 1). The results from right heart catheterization are summarized in Table 1. Right heart catheterization revealed severe PAH without left-to-right shunt. In addition, chest computed tomography and lung perfusion scintigraphy revealed no evidence of pulmonary thromboembolism. Serological examination was negative for connective tissue disease. Therefore, she was clinically diagnosed with PAH, and beraprost sodium (60 μg/day) and bosentan (125 mg/day) were initiated in March 2008. After 2–3 weeks of treatment, her 6MWD improved to 232 m (NYHA class II), and she was discharged 2 months later.

After leaving the hospital, she continued receiving regular outpatient treatment in our institute, but her body weight gradually increased and she developed severe right heart failure. She was rehospitalized 1 month later, presenting with worsening shortness of breath (NYHA class III) associated with a lower 6MWD of 169 m. Bosentan and beraprost sodium were increased to 187.5 mg/day and 120 μg/day, respectively, and sildenafil (60 mg/day) was added as adjunctive therapy. After 2 months of treatment, her 6MWD significantly improved to 430 m with NYHA class II, and she was discharged in July 2008 (Fig. 1).

Table 2. Changes in clinical parameters after tocilizumab therapy

	Before	1 month	3 months	6 months
6MWD (min)	400	495	N/A	480
NYHA class	II	II	I	I
RVSP (mmHg)	70	69	70	74
BNP (pg/ml)	341	122	202	244
UA (mg/dl)	8.1	6.7	6.6	6.4
CRP (mg/dl)	3.4	0.3	0.22	0.13
IL-6 (pg/dl)	15.2	406	464	346
RVDd (mm)	55	N/A	52	N/A
LVEF (%)	76	79	59	75

The 6MWD test was performed according to modified American Thoracic Society standards[12]
6MWD, 6-min walking distance; NYHA, New York Heart Association; RVSP, right ventricular systolic pressure; BNP, brain natriuretic peptide; UA, uric acid; CRP, C-reactive protein; IL-6, interleukin-6; RVDd, right ventricular diastolic diameter; LVEF, left ventricular ejection fraction; N/A, not available

Despite these treatments, she complained shortness of breath (NYHA class II dyspnea) and could not return to her previous work. Since she wished to return to work, she was rehospitalized 1 month later for tocilizumab treatment, as she strongly denied continuous intravenous epoprostenol therapy. Before starting tocilizumab therapy, her 6MWD was 400 m, RVSP 70 mmHg, BNP 341 pg/ml, UA 8.1 mg/dl, and CRP 3.4 mg/dl (Table 2). Serum IL-6 concentration was 15.2 pg/ml. She was started on 8 mg/kg tocilizumab once every 2 weeks, and after 1 month of hospitalization 6MWD, BNP, UA, and CRP were improved to 495 m, 122 pg/ml, 6.7 mg/dl, and 0.3 mg/dl, respectively. After leaving the hospital, she continued tocilizumab therapy once every 2 weeks as an outpatient. After 3 months of tocilizumab treatment, dyspnea improved (NYHA class I), and she was able to return to her previous work. After 6 months of treatment, 6MWD was 480 m without dyspnea, and BNP and UA were 244 pg/ml and 6.4 mg/dl, respectively (Table 2). Her general condition was sufficient for her to participate in all her activities of daily living, and she exhibited no adverse side effects while on tocilizumab.

The activity of Castleman's disease was well controlled by 12.5 mg/day prednisolone in 2007. The patient's chest computed tomography revealed swelling of axilla lymph node (12 mm in diameter); however, there was no uptake in the lymph node by gallium scintigraphy. Therefore, tocilizumab therapy was considered as a therapeutic option for PAH. During the treatment, there was no evidence of side effects or recurrence of Castleman's disease.

Discussion

Castleman's disease is linked to excessive immune stimulation by IL-6 or similar polypeptides, and has attracted atten-

tion because of its association with HIV and human herpes virus 8 (HHV-8) infections, both of which are also reported to play pathogenic role in PAH. The HHV-8 genome encodes a particularly potent viral IL-6 analogue and is associated with PAH in the setting of HIV/AIDS, Castleman's disease, and POEMS syndrome (Polyneuropathy, Organomegaly, Endocrinopathy, Monoclonal gammopathy, Skin changes).[10] Steroids have frequently been used as systemic treatment for Castleman's disease, with a response rate of 60%–70%, including 15%–20% complete response.[1] Recently, an additional benefit of treatment with neutralizing antibodies to IL-6 receptor has been reported in Castleman's disease, demonstrating clinical efficacy and symptom resolution.[5,13,14]

It is reported that the proinflammatory cytokine IL-6 is increased in the serum and lung from patients with idiopathic PAH.[15] Interleukin-6 is known to promote pulmonary vascular remodeling, and may play an important pathogenic role in the development and progression of pulmonary hypertension.[16] Furthermore, IL-10, a multifunctional anti-inflammatory cytokine, is reported to prevent monocrotaline-induced rat PAH as a result of its vascular protective property.[17]

We examined serum IL-6 levels during 6 months of tocilizumab treatment in this patient. Serum IL-6 concentration increased to 490 pg/ml by day 6, and was maintained during the follow-up period (Table 2). However, CRP levels decreased and normalized throughout the follow-up period. These findings suggest that tocilizumab effectively inhibits IL-6 signaling and the production of CRP.[18]

Although RVSP did not decrease during the follow-up period, 6MWD and NYHA functional class markedly improved on tocilizumab treatment. Moreover, serum UA concentration decreased to a normal level while on tocilizumab. Uric acid, the final product of purine degradation, has been shown to increase in hypoxic patients such as those with chronic heart failure, cyanotic congenital heart disease, and obstructive pulmonary disease. Serum UA levels increase in proportion to the clinical severity of pulmonary hypertension, and exhibit a strong, independent association with long-term mortality of patients with primary pulmonary hypertension.[19] The BNP level decreased after 1 month of tocilizumab treatment, although it had never been below 150 pg/ml even after 1–2 months of hospitalization before this treatment. Thereafter, the patient returned to her previous work, and BNP level improved on tocilizumab therapy and did not worsen during activities of daily living, as observed previously. Although RVSP did not decrease during the follow-up period, we speculate that earlier treatment with tocilizumab may have had an even more profound effect on remodeling on the pulmonary vascular bed.

There are some reports of successful therapy with tocilizumab in patients with Castleman's disease, though its efficacy in patients with PAH remains unknown. This is the first reported case of use of tocilizumab in addition to steroids and conventional PAH therapy in a patient with PAH associated with Castleman's disease. Our findings suggest that tocilizumab might be useful for the treatment of PAH associated with Castleman's disease.

References

1. Herrada J, Cabanillas F, Rice L, Manning J, Pugh W (1998) The clinical behavior of localized and multicentric Castleman disease. Ann Intern Med 128:657–662
2. Peterson BA, Frizzera G (1993) Multicentric Castleman's disease. Semin Oncol 20:636–647
3. Yoshizaki K, Matsuda T, Nishimoto N, Kuritani T, Taeho L, Aozasa K, Nakahata T, Kawai H, Tagoh H, Komori T, Kishimoto S, Hirano T, Kishimoto T (1989) Pathogenic significance of interleukin-6 (IL-6/BSF-2) in Castleman's disease. Blood 74:1360–1367
4. Oka H, Ikeda S, Koga S, Miyahara Y, Kohno S (2008) Atorvastatin induces associated reductions in platelet P-selectin, oxidized low-density lipoprotein, and interleukin-6 in patients with coronary artery diseases Heart Vessels 23:249–256
5. Nishimoto N, Kanakura Y, Aozasa K, Johkoh T, Nakamura M, Nakano S, Nakano N, Ikeda Y, Sasaki T, Nishioka K, Hara M, Taguchi H, Kimura Y, Kato Y, Asaoku M, Kumagai S, Kodama F, Nakahara H, Hagihara K, Yoshizaki K, Kishimoto T (2005) Humanized anti-interleukin-6 receptor antibody treatment of multicentric Castleman disease. Blood 106: 2627–2632
6. Nishimoto N, Nakahara H, Yoshio-Hoshino N, Mima T (2008) Successful treatment of a patient with Takayasu arteritis using a humanized anti-interleukin-6 receptor antibody. Arthritis Rheum 58:1197–1200
7. Nishimoto N, Yoshizaki K, Miyasaka N, Yamamoto K, Kawai S, Takeuchi T, Hashimoto J, Azuma J, Kishimoto T (2004) Treatment of rheumatoid arthritis with humanized anti-interleukin-6 receptor antibody: a multicenter, double-blind, placebo-controlled trial. Arthritis Rheum 50:1761–1769
8. Xiaohui L, Junbao D, Hongfang J, Bin G, Chaoshu T (2008) Sodium hydrosulfide alleviates pulmonary artery collagen remodeling in rats with high pulmonary blood flow. Heart Vessels 23:409–419
9. Simonneau G, Galie N, Rubin LJ, Langleben D, Seeger W, Domenighetti G, Gibbs S, Lebrec D, Speich R, Beghettei M, Rich S, Fishman A (2004) Clinical classification of pulmonary hypertension. J Am Coll Cardiol 43 suppl 12:5S–12S
10. Bull TM, Cool CD, Seris AE, Rai PR, Parr J, Neid JM, Geraci MW, Campbell TB, Voelkel NF, Badesch DB (2003) Primary pulmonary hypertension, Castleman's disease and human harpesvirus-8. Eur Respir J 22:403–407
11. Montani D, Achouh L, Marcelin AG, Viard J-P, Hermine O, Canioni D, Sitbon O, Simonneau G, Humbert M (2005) Reversibility of pulmonary arterial hypertension in HIV/HHV8-associated Castleman's disease. Eur Respir J 26:969–972
12. American Thoracic Society (2002) ATS statement guidelines for the six-minute walk test. Am J Respir Crit Care Med 166: 111–117
13. Beck JT, Hsu SM, Wijdenes J, Bataille R, Klein B, Vesole D, Hayden K, Jagannath S, Barlogie B (1994) Alleviation of systemic manifestations of Castleman's disease by monoclonal anti-interleukin-6 antibody. N Engl J Med 330:602–605
14. Nishimoto N, Sasai M, Shima Y, Nakagawa M, Matsumoto T, Shirai T, Kishimoto T, Yoshizaki K (2000) Improvement in Castleman's disease by humanized anti-interleukin-6 antibody therapy. Blood 95:56–61
15. Humbert M, Monti G, Brenot F, Sitbon O, Portier A, Grangeot-Keros L, Duroux P, Galanaud P, Simonneau G, Emilie D (1995) Increased interleukin-1 and interleukin-6 serum concentration in severe primary pulmonary hypertension. Am J Respir Crit Care Med 151:1628–1631
16. Steiner MK, Syrkina OL, Kolliputi N, Mark EJ, Hales CA, Waxman AB (2009) Interleukin-6 overexpression induced pulmonary hypertension. Circ Res 104:236–244
17. Ito T, Okada T, Miyashita H, Nomoto T, Nonaka-Sarukawa M, Uchibori R, Maeda Y, Urabe M, Mizukami H, Kume A, Takahashi M, Ikeda U, Shimada K, Ozawa K (2007) Interleukin-10 expression mediated by an adeno-associated virus vector prevents monocrotaline-induced pulmonary arterial hypertension in rats. Circ Res 101:734–741

18. Nishimoto N, Terao K, Mima T, Nakahara H, Takagi N, Kakehi T (2008) Mechanisms and pathologic significances in increase in serum interleukin-6 (IL-6) and soluble IL-6 receptor after administration of an anti-IL-6 receptor antibody, tocilizumab, in patients with rheumatoid arthritis and Castleman disease. Blood 112: 3959–3964

19. Nagaya N, Uematsu M, Satoh T, Kyotani S, Sakamaki F, Nkanishi N, Yamagishi M, Kunieda T, Miyatake K (1999) Serum uric acid levels correlate with the severity and the mortality of primary pulmonary hypertension. Am J Respir Crit Care Med 160: 487–492

Supplemental Material can be found at:
http://www.jbc.org/content/suppl/2010/07/27/M110.118653.DC1.html

THE JOURNAL OF BIOLOGICAL CHEMISTRY VOL. 285, NO. 41, pp. 31774–31782, October 8, 2010
© 2010 by The American Society for Biochemistry and Molecular Biology, Inc. Printed in the U.S.A.

BCR-ABL but Not JAK2 V617F Inhibits Erythropoiesis through the Ras Signal by Inducing p21$^{CIP1/WAF1}$*[S]

Received for publication, February 28, 2010, and in revised form, July 24, 2010 Published, JBC Papers in Press, July 27, 2010, DOI 10.1074/jbc.M110.118653

Masahiro Tokunaga[‡], Sachiko Ezoe[‡§1], Hirokazu Tanaka[‡], Yusuke Satoh[‡], Kentaro Fukushima[‡], Keiko Matsui[‡], Masaru Shibata[‡], Akira Tanimura[‡], Kenji Oritani[‡], Itaru Matsumura[‡¶], and Yuzuru Kanakura[‡]

From the [‡]Department of Hematology and Oncology, Osaka University Graduate School of Medicine, 2-2 Yamada-oka, Suita, Osaka 565-0871, the [§]Medical Center of Translational Research, Osaka University Hospital, Suita, Osaka 565-0871, and the [¶]Division of Hematology, Department of Internal Medicine, Kinki University School of Medicine, Osaka-Sayama, Osaka 589-8511, Japan

BCR-ABL is a causative tyrosine kinase (TK) of chronic myelogenous leukemia (CML). In CML patients, although myeloid cells are remarkably proliferating, erythroid cells are rather decreased and anemia is commonly observed. This phenotype is quite different from that observed in polycythemia vera (PV) caused by JAK2 V617F, whereas both oncogenic TKs activate common downstream molecules at the level of hematopoietic stem cells (HSCs). To clarify this mechanism, we investigated the effects of BCR-ABL and JAK2 V617F on erythropoiesis. Enforced expression of BCR-ABL but not of JAK2 V617F in murine LSK (Lineage$^-$Sca-1^{hi}CD117^{hi}) cells inhibited the development of erythroid cells. Among several signaling molecules downstream of BCR-ABL, an active mutant of N-Ras (N-RasE12) but not of STAT5 or phosphatidylinositol 3-kinase (PI3-K) inhibited erythropoiesis, while N-RasE12 enhanced the development of myeloid cells. BCR-ABL activated Ras signal more intensely than JAK2 V617F, and inhibition of Ras by manumycin A, a farnesyltransferase inhibitor, ameliorated erythroid colony formation of CML cells. As for the mechanisms of Ras-induced suppression of erythropoiesis, we found that GATA-1, an erythroid-specific transcription factor, blocked Ras-mediated mitogenic signaling at the level of MEK through the direct interaction. Furthermore, enforced expression of N-RasE12 in LSK cells derived from p53-, p16^{INK4a}/p19^{ARF}-, and p21$^{CIP1/WAF1}$-null/wild-type mice revealed that suppressed erythroid cell growth by N-RasE12 was restored only by p21$^{CIP1/WAF1}$ deficiency, indicating that a cyclin-dependent kinase (CDK) inhibitor, p21$^{CIP1/WAF1}$, plays crucial roles in Ras-induced suppression of erythropoiesis. These data would, at least partly, explain why respective oncogenic TKs cause different disease phenotypes.

Oncogenic tyrosine kinases (TKs)[2] such as BCR-ABL, FLT3-ITD, and JAK2 V617F are known to confer growth and/or survival advantage on hematopoietic cells, thereby causing hematologic malignancies (1–3). These gene alterations are supposed to occur at the hematopoietic stem cell (HSC) level (3, 4). Although these oncogenic TKs activate common downstream pathways including Ras/Raf/MEK/ERK, PI3-K/Akt, and STAT (1, 2, 5), their disease phenotypes are quite different: BCR-ABL is a causative gene of chronic myelogenous leukemia (CML) (1), FLT3-ITD of acute myeloid leukemia (AML) (2), and JAK2 V617F of myeloproliferative neoplasms including polycythemia vera (PV), essential thrombocythemia (ET) and primary myelofibrosis (PMF) (3). In patients with chronic-phase CML, anemia is a common feature in contrast to the marked leukocytosis in the peripheral blood. Also, bone marrow (BM) examination shows that erythroid islands are reduced in number and size despite the increased cellularity due to the granulocytic proliferation (6). This disease phenotype is totally different from that of PV, in which JAK2 V617F causes erythrocytosis together with the mild leukocytosis and thrombocytosis. Furthermore, in blast-phase CML, blast lineages are generally myeloid or lymphoid, and erythroid crisis is a rare incidence with a frequency no more than 5% (7, 8). These data suggest that, in contrast to the trilinear promoting activities of JAK2 V617F, BCR-ABL might not support the development of erythroid cells.

BCR-ABL activates several downstream pathways including Ras/Raf/MEK/ERK, STAT5, and PI3-K/Akt pathways (1, 4). Among them, we have previously shown that Ras plays crucial roles in the growth and survival of BCR-ABL-positive K562 cells, while STAT5 and PI3-K pathways contribute to their growth and survival to the only limited extent (9). In addition, although the role of STAT5 in BCR-ABL-mediated leukemogenesis remains controversial (10, 11), another group also reported that transformation of murine BM cells by BCR-ABL is blocked by dominant-negative Ras (12). Furthermore, Ras signaling was shown to be indispensable for the pathogenesis of CML in a murine BM transplantation model (13). Therefore, the activated Ras is considered to be essential for the pathogenesis of CML, and is also speculated to principally determine the disease phenotype of CML, that is, prominent proliferation of myeloid cells accompanied by the suppressed erythropoiesis.

* This work was supported by grants from the Ministry of Education, Science, Sports, and Culture and Technology of Japan.
[S] The on-line version of this article (available at http://www.jbc.org) contains supplemental Table S1 and Methods.
[1] To whom correspondence should be addressed. Tel.: 81-6-6879-3871; Fax: 81-6-6879-3879; E-mail: sezoe@bldon.med.osaka-u.ac.jp.
[2] The abbreviations used are: TK, tyrosine kinase; CML, chronic myelogenous leukemia; PV, polycythemia vera; HSC, hematopoietic stem cell; LSK, Lineage$^-$Sca-1^{hi}CD117^{hi}; BM, bone marrow; CDK, cyclin-dependent kinase; rh, recombinant human; TPO, thrombopoietin; rm, recombinant murine; EPO, erythropoietin; SCF, stem cell factor; G1ER, GATA-1/ER; 4-HT, 4-hydroxytamoxifen; Ab, antibody; HPRT, hypoxanthine phosphoribosyl transferase; pRb, retinoblastoma protein; PRAK, p38-regulated/activated protein kinase.

Downloaded from www.jbc.org at OSAKA UNIVERSITY, on May 12, 2011

Ras is constitutively activated by various oncogenic TKs or mutations of Ras itself in various malignant tumors. Although oncogenic (or constitutively activated) Ras was originally shown to transmit mitogenic and survival signals through Raf/MEK/ERK (14), recent studies have demonstrated that, like other oncogenic stimuli, it also induces growth inhibition/arrest in normal cells to prevent their malignant transformation. In general, this biological phenomenon is called "cellular senescence" and observed in various types of non-hematopoietic cells (15, 16). In addition, excessive Ras signaling was reported to inhibit erythropoiesis (17, 18), indicating the presence of a similar cellular response in hematopoietic cells. So far, oncogenic Ras has been shown to cause senescence through several signaling pathways other than Raf/MEK/ERK (15, 19–21). Also, several cell cycle regulatory molecules such as p53, p16^{INK4a}, p19^{ARF} and p21$^{CIP1/WAF1}$, have been shown to play central roles in oncogene-induced senescence (15, 19, 21).

In this report, we found that BCR-ABL but not JAK2 V617F, and among their downstream molecules, Ras but not STAT5 or PI3-K suppress erythropoiesis from murine LSK cells. As for this mechanism, we found that an erythroid-lineage specific transcription factor, GATA-1, blocks Ras-dependent growth and survival by inhibiting MEK1 activity through the direct interaction. Furthermore, we showed that a cyclin-dependent kinase (CDK) inhibitor, p21$^{CIP1/WAF1}$, plays crucial roles in Ras-induced suppression of erythropoiesis using p21$^{CIP1/WAF1}$-deficient hematopoietic cells.

EXPERIMENTAL PROCEDURES

Cytokines and Reagents—Recombinant human thrombopoietin (rhTPO) and recombinant murine interleukin-3 (rmIL-3) were provided by Kyowa Hakko Kirin (Tokyo, Japan). Recombinant human erythropoietin (rhEPO) and murine stem cell factor (rmSCF) were purchased from R & D Systems (Minneapolis, MN). Manumycin A was purchased from Merck KGaA (Darmstadt, Germany).

Plasmid Constructs and cDNAs—Expression vectors for GATA-1/ERT (G1ERT) and wild-type (WT) GATA-1 were described previously (22). Active forms of N-Ras (N-RasE12) (23) and STAT5A (1*6 STAT5A) (24), and membrane-targeted PI3-K catalytic subunit (p110^{CAAX}) (25) were subcloned into pMYs-IRES-EGFP, a retrovirus expression vector, which was kindly provided by Dr. T. Kitamura (University of Tokyo, Tokyo, Japan). pMSCV-IRES-GFP-p210-BCR-ABL is a generous gift from Dr. C. J. Eaves (Terry Fox Laboratory, Vancouver, BC, Canada) (26). The cDNA of JAK2 V617F was kindly provided by Dr. K. Shimoda (University of Miyazaki, Miyazaki, Japan) (27) and was subcloned into pMSCV-IRES-GFP.

Cell Lines and Cultures—A murine IL-3-dependent hematopoietic cell line, Ba/F3, was maintained in RPMI (nacalai tesque, Kyoto, Japan) supplemented with 10% fetal bovine serum (FBS) (Equitech-Bio, Kerrville, TX) and 0.3 ng/ml rmIL-3. NIH3T3 and 293T cells were cultured in Dulbecco's modified Eagle's medium (DMEM; nacalai tesque) supplemented with 10% FBS.

Preparation of Stable Transformants from Ba/F3—We introduced G1ERT into Ba/F3 cells by electroporation (250 V and 950 microfarads) and selected stably transfected clones by the culture with G-418 (1.0 mg/ml; Wako Pure Chemical Industries, Osaka, Japan). We further introduced pMYs-IRES-EGFP-N-RasE12 and obtained doubly transfected clones by sorting GFP-positive cells with BD FACSAria Cell-Sorting System (BD Biosciences, San Jose, CA). Their IL-3-independent growth and cell cycle were analyzed with or without the activation of GATA-1 by 4-hydroxytamoxifen (4-HT; Sigma-Aldrich). DNA contents of the cells were evaluated by staining with propidium iodide.

Luciferase Assays—Luciferase assays were performed with a Dual-Luciferase Reporter Assay System (Promega, Madison, WI) as previously described (22). As for assays using Ba/F3 cells, transfection was performed with Amaxa Nucleofector technology (Lonza, Cologne, Germany), followed by the measurement of luciferase activities after 24 h.

Immunoblotting and Coimmunoprecipitation Analyses—Preparation of cell lysates, immunoprecipitation, gel electrophoresis, and immunoblotting were performed according to the methods described previously (22, 28). Antibodies (Abs) and reagents were supplied by the manufacturers described in supplemental methods.

Glutathione S-transferase (GST) Pull-down Assays—GST pull-down assays were performed as previously reported (22).

Animals—The congenic C57BL/6J mice were purchased from Clea Japan, Inc. (Tokyo, Japan). B6.129-Cdkn2a^{tm1Rdp} (p16^{INK4a}/p19^{ARF}-null) mice and p53-null mice were kindly provided by Technology Transfer Center National Cancer Institute (Rockville, MD) and Dr. N. Nishimoto (Wakayama Medical University, Wakayama, Japan), respectively. B6.129S2-Cdkn1a^{tm1Tyj}/J (p21$^{CIP1/WAF1}$-null) mice were purchased from The Jackson Laboratory (Bar Harbor, ME). The experimental designs of this study were approved by the Institutional Animal Care and Use Committee at Osaka University Graduate School of Medicine.

Separation of Murine Hematopoietic Progenitors—Murine BM cells were flushed from both femora and tibiae, and progenitors were concentrated by anti-mouse CD117 MicroBeads and autoMACS Pro Separator (Miltenyi Biotec, Bergisch Gladbach, Germany). To isolate LSK (Lineage$^-$Sca-1^{hi}CD117^{hi}) cells, selected progenitors were stained with phycoerythrin-conjugated (PE-conjugated) monoclonal Abs against murine lineage markers (CD3e (145–2C11), CD45R/B220 (RA3–6B2), Gr-1 (RB6–8C5), CD11b (M1/70), and TER-119 (TER-119)), fluorescein isothiocyanate-conjugated (FITC-conjugated) anti-Sca-1 Ab (E13–161.7), and allophycocyanin-conjugated (APC-conjugated) anti-CD117 Ab (2B8), and isolated by FACSAria. All Abs were purchased from BD Biosciences.

Preparation of Retrovirus Particles—Preparation of retrovirus particles was performed as described previously (29) (see supplemental methods).

Retrovirus Transfection into Murine BM Progenitors—Isolated LSK cells were precultured overnight in DMEM supplemented with 10% FBS, rmSCF (100 ng/ml), and rhTPO (100 ng/ml). Then, the cells were seeded on 24-well tissue plates coated with RetroNectin (TaKaRa Bio Inc., Shiga, Japan), infected with each viral supernatant by spinoculation, and cultured in the same medium containing 10% FBS, protamine sulfate (10 μg/ml; Sigma-Aldrich), rmSCF (50 ng/ml), and rhTPO (50 ng/ml). After 48 h of culture, retrovirus-transduced GFP$^+$

Downloaded from www.jbc.org at OSAKA UNIVERSITY, on May 12, 2011

cells were sorted with FACSAria and were subjected to colony assays or stromal coculture.

Colony Assays—Cells were plated at the indicated density in methylcellulose medium (MethoCult; Stem Cell Technologies, Vancouver, BC, Canada) supplemented with the indicated growth factors. Cells were incubated with 5% CO_2 at 37 °C, and the numbers of colonies were counted after the indicated days.

Stromal Coculture—A murine BM stromal cell line, MS-5, was cultured in minimum essential medium (MEM) α (Invitrogen, Carlsbad, CA) with 10% FBS and prepared in 24-well tissue plates 1 day before the seeding. The sorted GFP$^+$ progenitors were seeded (1.5×10^3 cells/well) on the monolayer of MS-5 and cocultured in 2 ml of MEMα supplemented with 10% FBS, rmSCF (50 ng/ml), and rhEPO (3 units/ml). Five days after the initiation of coculture, hematopoietic cells were harvested and stained with PE-conjugated anti-CD45 (30-F11) Ab, and APC-conjugated anti-CD11b (M1/70) or anti-TER-119 (TER-119) Ab (all of them from BD Biosciences). To evaluate the phosphorylation status of ERK1/2, we used BD Phosflow technology (BD Biosciences). The harvested cells were further incubated in DMEM containing 2% FBS without cytokines for 4 h, then fixed, permeabilized, and stained with Alexa Fluor®647-conjugated anti-ERK1/2 (pT202/pY204) Ab (BD Biosciences) according to the manufacturer's recommendation.

Flow Cytometric Analyses—Flow cytometric analyses were performed using BD FACSCanto II (BD Biosciences). The data analyses were done with BD FACSDiva software (BD Biosciences) or FlowJo software (TreeStar, Ashland, OR).

Immunofluorescence Microscopy—5×10^4 of the transduced cells were cytospun onto microscope slides, fixed in 2% paraformaldehyde, and permeabilized in 1% Nonidet P-40 in PBS. After the incubation in blocking buffer (1 mg/ml of γ-globulin in PBS), the slides were incubated with a monoclonal Ab against p16^{INK4a} (F-12) or p19^{ARF} (5-C3–1) (both from Santa Cruz Biotechnology, Santa Cruz, CA). The slides were then incubated with an Alexa Fluor®546-conjugated secondary antibody (goat anti-mouse IgG for p16^{INK4a}, or goat anti-rat IgG for p19^{ARF}), followed by the staining of nuclei with Hoechst 33342 (all from Invitrogen). The slides were mounted in Fluoromount (Diagnostic BioSystems, Pleasanton, CA) before viewing on a LSM 5 PASCAL microscope (Carl Zeiss, Oberkochen, Germany).

Semiquantitative RT-PCR—Total RNA was isolated from 5×10^3 of the transduced cells using RNeasy Mini Kit (Qiagen, Hilden, Germany) and converted to cDNA by SuperScript III First Strand Synthesis System (Invitrogen). PCR was performed using Ampli Taq Gold (Applied Biosystems, Carlsbad, CA) with primers described in supplemental Table S1.

Real-time RT-PCR—Quantitative real-time RT-PCR was performed using FastStart Universal SYBR Green Master (Roche Diagnostics GmbH, Mannheim, Germany) and PRISM 7900HT (Applied Biosystems). Amplified signals were normalized to the levels of hypoxanthine phosphoribosyl transferase (HPRT). The primer sequences are described in supplemental Table S1.

BM Samples from CML Patients—BM samples were obtained from three patients with newly diagnosed chronic-phase CML. CD34$^+$ cells were separated using the MACS immunomagnetic separation system, and were subjected to colony assays. All BM samples were obtained after receiving written informed consent in accordance with the Declaration of Helsinki, and this study protocol was approved by the institutional review board of Osaka University Hospital.

Statistical Methods—Statistical analyses were carried out by standard Student *t* tests. Error bars used throughout indicate S.D.

RESULTS

BCR-ABL but Not JAK2 V617F Inhibits the Development of Erythroid Cells—To examine the effects of BCR-ABL on erythropoiesis, we first introduced p210-BCR-ABL into murine LSK cells using the retrovirus vector harboring GFP as a reporter gene. After 48 h, GFP$^+$ cells were sorted and cocultured with a murine BM stromal cell line, MS-5, in the presence of rmSCF and rhEPO for 5 days. As compared with mock-transduced cells, the proportion of CD45^{low}TER-119$^+$ erythroid cells was reduced in BCR-ABL-transduced cells significantly (Fig. 1*A*). We also examined the effects of JAK2 V617F on erythropoiesis with the same strategy and found that JAK2 V617F did not reduce the proportion of erythoroid cells. In colony assays, BCR-ABL significantly decreased the number of burst-forming units-erythroid (BFU-E), while it increased the number of myeloid colonies (Fig. 1*B*). On the other hand, JAK2 V617F did not reduce the number of BFU-E. These data indicate that BCR-ABL but not JAK2 V617F inhibits the development of erythroid cells from murine hematopoietic progenitors.

Oncogenic Ras Inhibits Erythropoiesis Downstream of BCR-ABL—BCR-ABL activates mainly Ras/Raf/MEK/ERK, JAK2/STAT5, and PI3-K/Akt pathways. Next, to examine the roles of these pathways in erythropoiesis, we transduced LSK cells with an active form of each signal transduction molecule: N-RasE12 for an active form of N-Ras, 1*6 STAT5A for STAT5, and p110^{CAAX} for PI3-K. Compared with Mock, 1*6 STAT5A and p110^{CAAX} increased total erythroid cell numbers by 2.8- and 1.9-fold, respectively (both, $p < 0.05$), while the proportion of erythroid cells was scarcely influenced by both molecules due to the increase in total cell numbers (Fig. 2, *A* and *B*). In contrast, N-RasE12 remarkably reduced not only the frequency (Fig. 2*A*) but also the number of erythroid cells (0.28-fold) (Fig. 2*B*), while it significantly increased the number of CD11b$^+$-myeloid cells (Fig. 2*C*). We also performed colony assays using N-RasE12- or Mock-transduced LSK cells. As shown in Fig. 2*D*, N-RasE12 significantly reduced the number of BFU-E (average colony numbers from 1.0×10^3 cells input: Mock-transduced cells, 9.7; N-Ras-transduced cells, 0.33) ($p < 0.01$).

BCR-ABL Activates Ras Signal More Intensely than JAK2 V617F—Next, we tried to clarify why JAK2 V617F did not suppress erythropoiesis, because it has been reported to activate Ras as well as BCR-ABL (5). For this purpose, we introduced JAK2 V617F and BCR-ABL into murine LSK cells, cocultured them with MS-5, and evaluated the Ras activity by expediently measuring the phosphorylation status of ERK1/2 after 4-h starvation of cytokines. As shown in Fig. 2*E*, ERK1/2 was more intensely phosphorylated (activated) in cells transduced with BCR-ABL than in those with JAK2 V617F. We also examined the phosphorylation status of ERK1/2 in CML patients' blood

Downloaded from www.jbc.org at OSAKA UNIVERSITY, on May 12, 2011

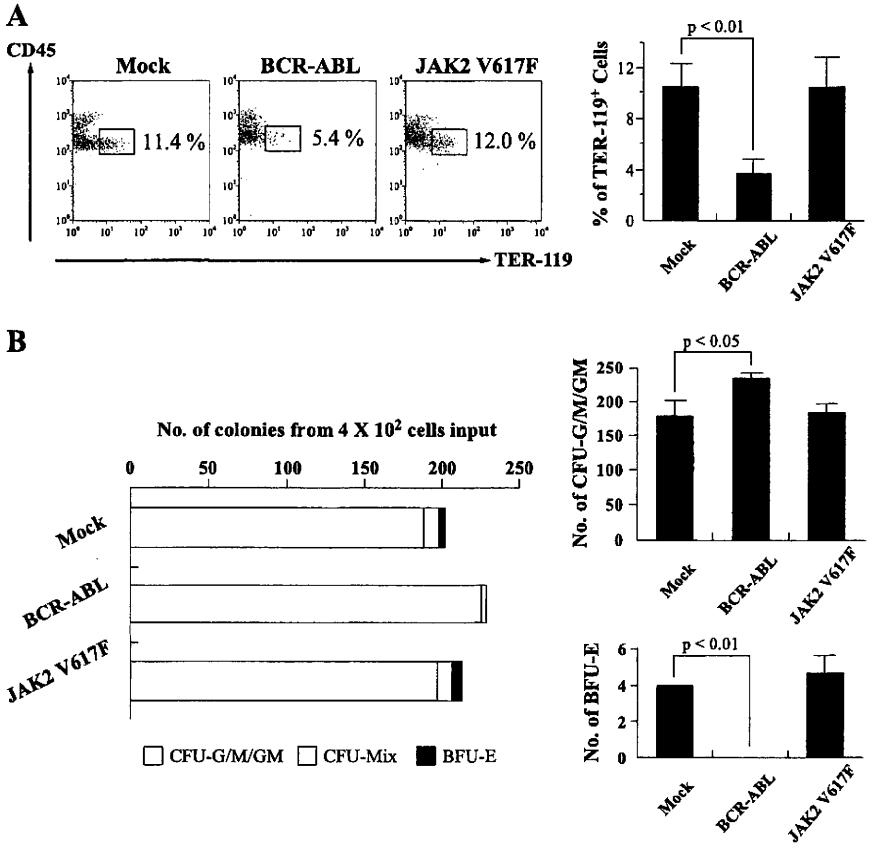

FIGURE 1. **Effects of oncogenic TKs on proliferation of erythroid cells.** *A*, after infection of retrovirus expressing Mock, BCR-ABL, or JAK2 V617F into murine LSK cells, GFP$^+$ cells were sorted and cocultured with MS-5 in the presence of rmSCF and rhEPO. After 5-day cultures, expression of CD45 and TER-119 was analyzed by flow cytometry (*left panels*). The proportions of CD45^{low}TER-119$^+$ cells are shown in the *right bar graph* (n = 3). *B*, respective retrovirus-transduced LSK cells were seeded at a density of 2.0 × 10^2 cells/35-mm dish in methylcellulose medium containing rmSCF, rmIL-3, rmIL-6, rhTPO, and rhEPO. Colony numbers were counted after 9 days. Representative colony numbers (*left*) and myeloid/erythroid colony numbers (*right*, n = 3) are shown. BFU-E, burst-forming units-erythroid; CFU-G/M/GM, colony-forming unit-granulocyte/macrophage/granulocyte-macrophage.

cells treated with manumycin A, a potent farnesyltransferase inhibitor which selectively suppresses Ras, or vehicle only. As shown in Fig. 2*F*, phosphorylation of ERK was reduced by Ras inhibition, indicating that BCR-ABL activates ERK through the activation of Ras. These data indicate that different growth status of erythroid cells between these TKs might result from the preferential activation of Ras signal by BCR-ABL.

Suppression of Ras Signal Ameliorates the Inhibition of Erythropoiesis Caused by BCR-ABL—Furthermore, to make sure that suppressed erythropoiesis caused by BCR-ABL is due to the activation of Ras signal, we examined the effects of Ras-inhibition on erythroid colony formation of BCR-ABL expressing cells. CD34$^+$ cells were separated from BM samples of three patients with newly diagnosed chronic-phase CML. They were then cultured in methylcellulose medium containing rhSCF, rhIL-3, and rhEPO, with or without manumycin A. Complete blockage of Ras signal by supplement of sufficient dose (10 μM) of manumycin A eradicated erythroid colony formation (data not shown). However, as shown in Fig. 2*G*, the number of erythroid colonies was restored by low doses of manumycin A in all three patients, though there was some difference in degree. This result, actually in primary CML cells, supports our model that, although Ras is indispensable for erythroid cell survival, excessive Ras signal downstream of BCR-ABL rather inhibits erythroid cell proliferation.

GATA-1 Inhibits Ras-dependent Cell Proliferation and Survival—As described above, oncogenic Ras signaling promoted the proliferation of myeloid cells, but inhibited that of erythroid cells. To elucidate the mechanisms underlying the different responses to oncogenic Ras between the two lineages, we examined the effects of GATA-1, which is expressed in erythroid cells but not in myeloid cells, on Ras signal. For this purpose, we transduced N-RasE12 and G1ERT, a chimera gene consisting of full-length GATA-1 and the mutated ligand-binding domain of estrogen receptor, into Ba/F3 cells, which was named Ba/F3/N-RasE12/G1ERT. G1ERT reveals GATA-1 activity in response to 4-HT as previously reported (22). As shown in Fig. 3*A*, N-RasE12 enabled this clone to proliferate and survive independently of IL-3. However, when GATA-1 activity was induced by 4-HT treatment, N-RasE12-dependent cell growth was completely suppressed (Fig. 3*A*). In agreement with this result, the proportion of growing cells in S-G2/M phase was reduced by 4-HT treatment from 36% to 8% in DNA contents analysis (Fig. 3*B*). Furthermore, 4-HT treatment induced apoptosis in 78% of cells, which was detected as a subdiploid fraction. From these results, we speculated that GATA-1 might inhibit oncogenic Ras activities, which transmit proliferation and survival signals.

GATA-1 Suppresses MEK Activity—Ras signal is known to be transmitted to the nucleus through Raf, MEK, and ERK in this order. To identify which molecule was inhibited by GATA-1 in this pathway, we performed luciferase assays using a reporter gene for ERK (3 × AP-1-Luc) in NIH3T3 and Ba/F3 cells. As shown in Fig. 4, *A* and *B*, GATA-1 significantly reduced the N-Ras- and MEK1-induced AP-1-luciferase activities almost to the baseline levels (*white boxes*), which indicates that GATA-1 inhibits Ras signal at the level or downstream of MEK. Next, we examined the phosphorylation status of MEK1/2 and ERK1/2 in Ba/F3/N-RasE12/G1ERT cells by immunoblot analysis. As shown in Fig. 4*C*, both MEK1/2 and ERK1/2 were phosphorylated by N-RasE12 even under the culture without IL-3, which was suppressed by 4-HT in a time-dependent manner. This

Downloaded from www.jbc.org at OSAKA UNIVERSITY, on May 12, 2011

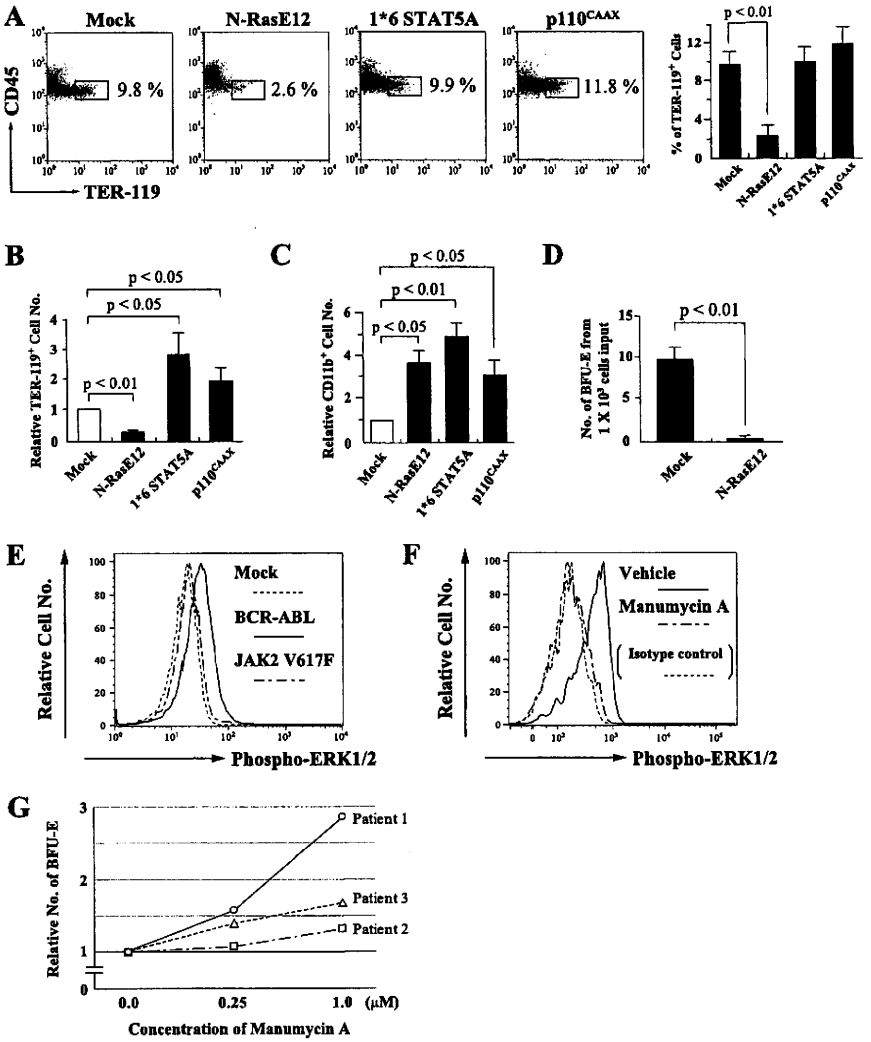

FIGURE 2. **Roles of downstream molecules of oncogenic TKs in erythropoiesis.** *A–C*, LSK cells each transfected with the indicated gene were cocultured with MS-5 in the medium containing rmSCF and rhEPO. After 5 days, expression of CD45 and TER-119 was analyzed by flow cytometry (*A*, *left panels*) and the proportions of CD45^{low}TER-119$^+$ cells are shown (*A*, *right bar graph*, $n = 3$). Numbers of the TER-119$^+$ cells were calculated by multiplication of the frequencies and total cell numbers. Relative numbers to Mock are shown (*B*). Relative CD11b$^+$ myeloid cell numbers are shown (*C*). *D*, retrovirus-infected LSK cells were seeded at a density of 5.0×10^2 cells/dish in methylcellulose medium containing rmSCF, rmIL-3, and rhEPO. The numbers of BFU-E were counted after 8 days ($n = 3$). *E*, LSK cells, each transfected with Mock, BCR-ABL, or JAK2 V617F, were further incubated without cytokines after the coculture with MS-5, and the phosphorylation status of ERK1/2 was analyzed using Phosflow technology. *F*, after 5-h incubation of CML patients blood mononuclear cells with manumycin A (7 μM) or vehicle, the phosphorylation status of ERK1/2 was analyzed. *G*, CD34$^+$ cells were separated from BM samples of three CML patients, and seeded in methylcellulose medium containing rhSCF, rhIL-3, and rhEPO, with manumycin A at the indicated concentrations or vehicle. The numbers of BFU-E were counted after 9 days, and shown as relative numbers to vehicle in each patient.

result implies that GATA-1 suppresses Ras signal at the level or upstream of MEK. Together with the results from luciferase assays, it was speculated that GATA-1 would inhibit MEK activity.

GATA-1 Blocks the Ras Signal through Its Direct Interaction with MEK1—To clarify how GATA-1 inhibits MEK activities, we examined the interaction between GATA-1 and MEK1. First, we transfected 293T cells with hemagglutinin-tagged (HA-tagged) GATA-1 and/or Flag-tagged MEK1. Total cellular lysates were prepared after 36 h, and GATA-1 was immunoprecipitated with the anti-HA Ab and MEK1 with the anti-Flag Ab. As shown in Fig. 4*D*, immunoblotting with the anti-Flag Ab showed that MEK1 was coimmunoprecipitated with GATA-1 only when both molecules were cotransduced. Also, immunoblotting with the anti-HA Ab showed that GATA-1 was coimmunoprecipitated with MEK1.

Next, to examine whether endogenous GATA-1 and MEK interact in primary erythroid cells, we performed a coimmunoprecipitation analysis using murine BM erythroid cells: Cells positive for CD71 (transferrin receptor), which is expressed at high levels on erythroid progenitors, were purified using the MACS immunomagnetic separation system. Total cellular lysate was prepared and subjected to immunoprecipitation with an anti-GATA-1 Ab or rat isotype IgG. Fig. 4*E* shows that MEK is coimmunoprecipitated with GATA-1, indicating that these molecules actually interact with each other in primary erythroid cells.

Finally, we investigated whether MEK1 directly binds to GATA-1 *in vitro* by GST pull-down assays. After verifying the quality and quantity of GST-MEK1 fusion protein by Coomassie Brilliant Blue staining (data not shown), we analyzed the binding between GST-MEK1 and *in vitro*-translated GATA-1. As shown in Fig. 4*F*, GST-MEK1 but not GST alone, bound to ^{35}S-labeled GATA-1 *in vitro*.

Together with the results of Fig. 4, *A–C*, we proved the following two facts: GATA-1 inhibits MEK activation; GATA-1 and MEK interact with each other in primary erythroid progenitors. From these facts, we speculated that GATA-1 blocks Ras signal at least partly through the direct interaction with MEK1.

Oncogenic Ras Induces Suppression of Erythropoiesis through the Induction of p21$^{CIP1/WAF1}$—In addition to the functions to deliver mitogenic and anti-apoptotic signals (14), Ras paradoxically causes growth arrest (senescence) in normal cells through several cell cycle regulatory molecules such as p53, p16^{INK4a}, p19^{ARF}, and p21$^{CIP1/WAF1}$ (15, 21). Among them, p53 is a tumor-suppressor and acts as a pivotal regulator of these responses (15, 16, 19, 21). p19^{ARF} is a splicing variant of p16^{INK4a} and inhibits the function of H/MDM2, which pro-

Downloaded from www.jbc.org at OSAKA UNIVERSITY, on May 12, 2011

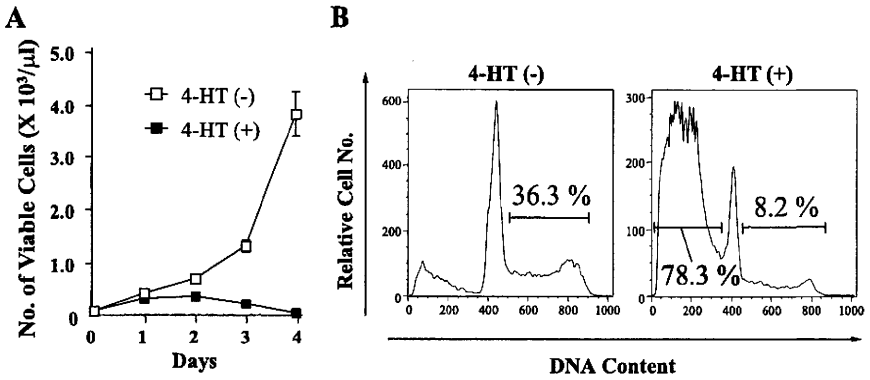

FIGURE 3. **Inhibition of Ras-dependent cell proliferation and survival by GATA-1.** *A*, Ba/F3/N-RasE12/G1ERT cells were seeded at a density of 100/μl and cultured in RPMI supplemented with 1% FBS without IL-3 in the presence or absence of 1 μM 4-HT. Total numbers of viable cells were counted by trypan blue dye exclusion method on the indicated days. The results are shown as means ± S.D. of triplicate cultures. *B*, after 48 h of culture, DNA contents of 4-HT-treated or untreated cells were examined by propidium iodide staining. The proportions of cells in S-G2/M phase and subdiploid fraction are shown, respectively.

motes degradation of p53 (30). p16^{INK4a} is a member of the INK4 family of CDK inhibitors, which causes cell cycle arrest at G1 phase by inhibiting CDK4/6 activities (30). Meanwhile, p21$^{CIP1/WAF1}$ is a member of the Cip/Kip family of CDK inhibitors and also induces G1 arrest by inhibiting CDK2 activities. In this report, we next examined their roles in N-RasE12-induced suppression of erythropoiesis.

At first, we examined the effects of N-RasE12 on the expression of p16^{INK4a}, p19^{ARF}, and p21$^{CIP1/WAF1}$ by semiquantitative/real-time RT-PCR analyses or immunofluorescence. As shown in Fig. 5*A* and *B*, the expression of p16^{INK4a} and p19^{ARF} was induced in N-RasE12-transduced LSK cells both in mRNA and protein levels. Also, the expression of p21$^{CIP1/WAF1}$ was increased by nearly 2-fold in N-RasE12-transduced LSK cells compared with mock-transduced LSK cells (Fig. 5*C*), suggesting that the up-regulated p16^{INK4a}, p19^{ARF}, and/or p21$^{CIP1/WAF1}$ might be involved in N-RasE12-induced suppression of erythropoiesis.

To further analyze the roles of these molecules, we next introduced N-RasE12 into LSK cells isolated from p16^{INK4a}/p19^{ARF} double knock-out (KO) mice, cocultured them with MS-5, and examined the development of erythroid cells by flow cytometry. As shown in Fig. 6*A*, the frequency of CD45^{low}TER-119^{+} erythroid cells was a little lower in N-RasE12-transduced double KO cells than in N-RasE12-transduced WT cells (WT 1.8% *versus* double KO 0.8%) (*upper panels*). In addition, although the number of these erythroid cells was slightly restored in N-RasE12-transduced double KO cells compared with N-RasE12-transduced WT cells (*lower graph*), this difference was not significant.

We also introduced N-RasE12 into LSK cells isolated from p21$^{CIP1/WAF1}$-null mice. As observed in the other experiments, N-RasE12 reduced the proportion of CD45^{low}TER-119^{+} erythroid cells both in WT and p21$^{CIP1/WAF1}$-null LSK cells (Fig. 6*B*, *upper panels*). However, p21$^{CIP1/WAF1}$ deficiency partially, but significantly, restored the proportion of this fraction from 3.0 to 5.2%. In addition, surprisingly, N-RasE12 increased the number of erythroid cells in p21$^{CIP1/WAF1}$-null LSK cells compared with mock-transduced LSK cells (Fig. 6*C*, *lower graph*), indicating that p21$^{CIP1/WAF1}$ is a major regulator of N-RasE12-induced suppression of erythropoiesis.

Because the expression of p21$^{CIP1/WAF1}$ is regulated in p53-dependent and independent manners (31–33), we finally investigated the roles of p53 in N-RasE12-induced suppression of erythropoiesis with the similar experiment. As shown in Fig. 6*C*, the proportion and number of erythroid cells in mock-transduced LSK cells were reduced by p53 deficiency. In addition, p53 deficiency did not cancel the inhibition of erythroid cell development by N-RasE12. Together, these results indicate that N-RasE12 inhibits erythropoiesis through p21$^{CIP1/WAF1}$ in a p53-independent manner.

DISCUSSION

We here found that BCR-ABL suppresses erythroid cell proliferation. This finding is largely consistent with clinical features of CML, in which anemia is commonly observed and erythroid blast crisis is a rare event. Also, we found that constitutively activated Ras, but not PI3-K or STAT5, inhibits erythropoiesis and that a farnesyltransferase inhibitor, manumycin A, restores erythroid colony formation of CML patients BM cells at relatively low concentrations. These results strongly indicate that Ras is a negative regulator of erythropoiesis downstream of BCR-ABL. So far, functions of Ras in normal erythropoiesis are controversial. It was reported that Ras signaling was essential for development of erythroid progenitors (34, 35). In contrast, H-Ras$^{-/-}$, N-Ras$^{-/-}$, and double KO (H-Ras$^{-/-}$ N-Ras$^{-/-}$) mice had no apparent hematopoietic abnormality, indicating that Ras is dispensable for normal erythropoiesis (36, 37). Regarding the roles of oncogenic Ras in erythropoiesis, it was shown that oncogenic H-Ras blocks terminal erythroid differentiation (38), and that enforced expression of an active mutant of N-Ras in primitive hematopoietic cells inhibits proliferation of erythroid cells (17, 18). Our results indicate that the excessive Ras signal would inhibit erythropoiesis, though Ras signal might be to some extent necessary for erythroid cell survival. Ras is mutated in a significant proportion of cases with acute myeloid leukemia and myelodysplastic syndromes (39), or constitutively activated by various oncogenic TKs, including FLT3-ITD (2), c-KIT D816V (40), and TEL-PDGFRB (41). So, anemia observed in these hematologic malignancies also might be, at least partly, attributed to the constitutively activated Ras signal. However, in this study, JAK2 V617F slightly enhanced erythropoiesis as observed in patients with PV, whereas its downstream pathways including Ras, PI3-K, and STAT5 are common to BCR-ABL (1, 5). As for this difference, we here found that JAK2 V617F does not activate Ras signal so strongly as BCR-ABL. Also, it was speculated that JAK2 V617F would utilize mainly STAT5 to promote erythropoiesis in PV patients. Although Ras has some isoforms, we focused on N-Ras,

Downloaded from www.jbc.org at OSAKA UNIVERSITY, on May 12, 2011

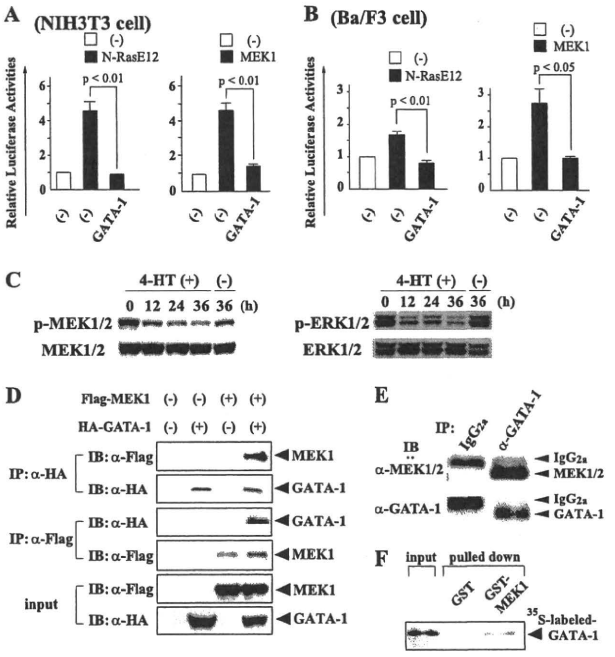

FIGURE 4. **GATA-1 blocks the Ras/Raf/MEK/ERK pathway through its direct interaction with MEK1.** *A*, NIH3T3 cells (2×10^5 cells seeded in 60-mm dish) were transfected with the indicated expression vectors and the reporter gene (3 × AP-1-Luc) together with pRL-CMV. After 12 h, the cells were serum-deprived for 24 h, then lysed, and subjected to the measurement of the firefly and *Renilla* luciferase activities. The relative firefly luciferase activities normalized by the *Renilla* luciferase activities are shown as means ± S.D. of three separate experiments. *B*, Ba/F3 cells (2×10^6 cells) were transfected with the same vectors as Fig. 4*A* using Amaxa Nucleofector technology. After 24 h of culture, the cells were lysed and subjected to the measurement of the luciferase activities. *C*, Ba/F3/N-RasE12/G1ERT cells cultured in RPMI supplemented with 1% FBS were treated with 1 μM 4-HT or vehicle. Total cellular lysates were prepared at the indicated time and subjected to immunoblotting with the indicated Abs. The filters were reprobed with corresponding Abs to confirm that the equal amounts of the proteins were loaded. *D*, coimmunoprecipitation analyses were performed using 293T cells transfected with HA-tagged GATA-1 and/or Flag-tagged MEK1 as indicated. *IP*, immunoprecipitation; *IB*, immunoblotting; α, anti. *E*, total cellular lysate was prepared from murine BM CD71$^+$ cells. Immunoprecipitation and immunoblot analyses were performed with the indicated antibodies. F. The *in vitro* binding between GATA-1 and MEK1 was examined by GST pull-down assays. ^{35}S-labeled GATA-1 was incubated with GST-MEK1 bound to glutathione-Sepharose beads, and the binding complex was separated by gel electrophoresis and subjected to autoradiography.

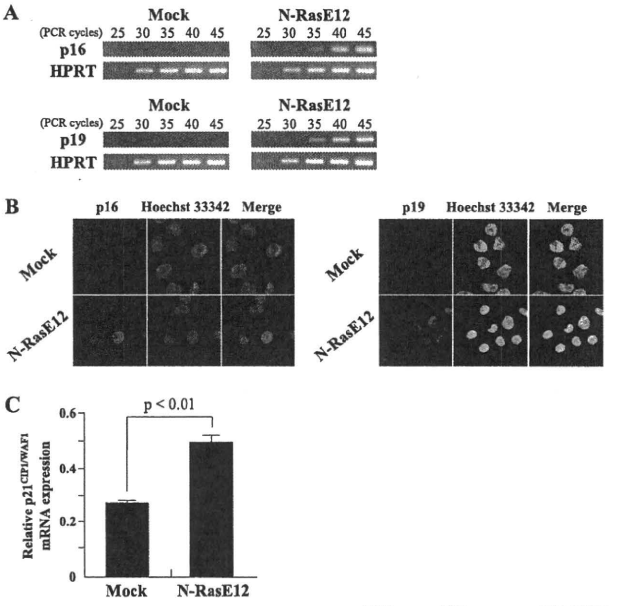

FIGURE 5. **Increase in expression levels of p16^{INK4a}, p19^{ARF}, and p21$^{CIP1/WAF1}$ by oncogenic Ras.** *A–C*, LSK cells transfected with Mock or N-RasE12 were cultured with rmSCF, rmIL-3, and rhEPO for 2 days. Total RNA was isolated from GFP$^+$ cells, and the expression levels of p16^{INK4a} and p19^{ARF} were analyzed by semiquantitative RT-PCR (*A*). Immunofluorescence staining of p16^{INK4a} and p19^{ARF} localizations (*red*) in Hoechst 33342-stained nuclei of GFP$^+$ cells are shown (magnification, 630×) (*B*). The expression levels of p21$^{CIP1/WAF1}$ were analyzed by real-time RT-PCR. The results are normalized to the levels of HPRT gene and shown as means ± S.D. ($n = 3$) (*C*).

because, in myeloid malignancies, N-Ras mutations are more frequent than K-Ras, whereas H-Ras mutations are rare (39, 42–44). It is predictable that activated N-Ras has stronger leukemogenic potential than activated H-Ras or K-Ras.

In contrast to the negative role of oncogenic Ras in erythropoiesis, Ras activation prominently enhanced the development of myeloid cells from LSK cells as observed in CML patients. To clarify the mechanism through which the active form of Ras plays different roles in the growth of hematopoietic cells according to the cell lineages (*i.e.* inhibition of erythropoiesis but promotion of myelopoiesis), we examined the role of GATA-1, which is a transcription factor mainly expressed in erythroid and megakaryocytic cells but not in myeloid cells. Ras-induced suppression of erythropoiesis can be considered to result from inhibition of proliferation of already committed erythroid progenitors, and blockage of commitment into erythroid lineage from HSCs. In this study, we found that GATA-1 inhibits MEK activity and suppresses the Ras-dependent proliferation of GATA-1-posistive cells. GATA-1 is necessary in the post-commitment stages of erythroid and megakaryocytic development, and is highly expressed after the commitment into megakaryocyte-erythrocyte progenitors (MEPs), but is scarcely expressed in HSCs (45). So, it is unlike that the interaction between GATA-1 and MEK1 is associated with the lineage determination of HSCs. On the other hand, recent reports showed that suppression of erythroid cell development by H-, K-, and N-Ras occurs at later stages of differentiation (18, 38, 46). These data are consistent with our result that GATA-1 interacts with MEK1, thereby inhibiting Ras-mediated mitogenic signals.

However, this result raises a question where these molecules interact together in the cells because GATA-1 is located in the nucleus and MEK is in the cytoplasm (47). As an explanation it was previously reported that MEK contains a nuclear export signal in its N-terminal domain, indicating that MEK is translocated to the nucleus upon mitogenic stimulation and then goes back to the cytoplasm after transduction of its signal (48). So, GATA-1 is supposed to interact with MEK1 in the nucleus, thereby inhibiting its activity. This hypothesis that GATA-1 would inhibit MEK activities is also contradictory to the fact that platelet counts are often elevated in CML patients, because MEK has been shown to be important for the maturation (polyploidization) of megakaryocytes, in which GATA-1 is highly expressed as well as in erythroid cells. Regarding this issue, Jacquel *et al.* reported that PMA-induced megakaryocytic maturation is only partly dependent on the MEK/ERK pathway and suggested the involvement of other pathways such

Downloaded from www.jbc.org at OSAKA UNIVERSITY, on May 12, 2011

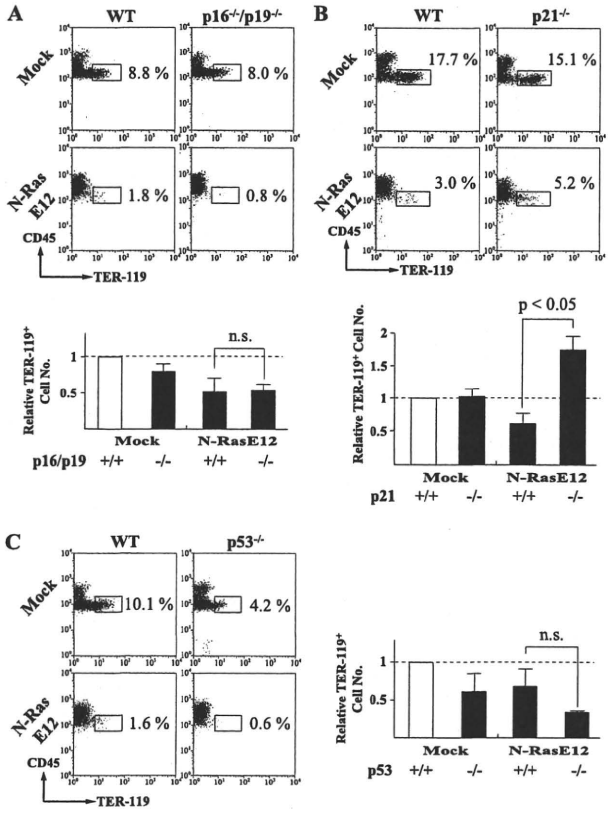

FIGURE 6. **p21$^{CIP1/WAF1}$ but not p53 or p16^{INK4a}/p19^{ARF} mediates oncogenic Ras-induced suppression of erythropoiesis.** *A–C*, LSK cells were isolated from BM of the indicated mice. After retrovirus infection, GFP$^+$ cells were sorted and cocultured with MS-5 in the presence of rmSCF and rhEPO. The expression of CD45 and TER-119 was analyzed after 5 days. Bar graphs represent the relative TER-119$^+$ cell numbers normalized to mock-transduced WT cells (*dashed lines*). *n.s.*, not significant.

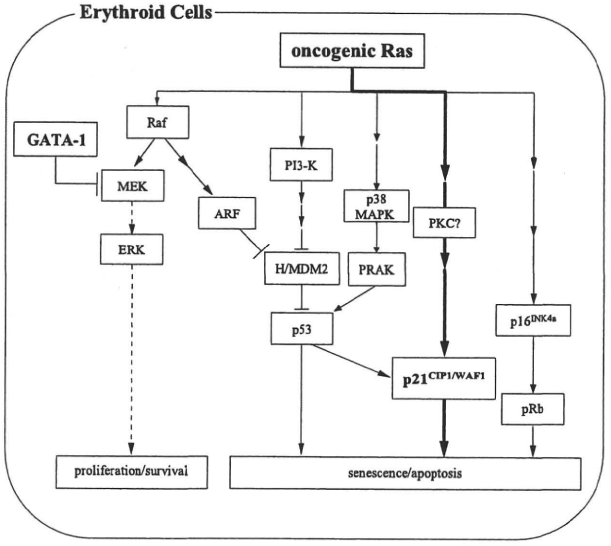

FIGURE 7. **A proposed model for oncogenic Ras-induced suppression of erythropoiesis.** Oncogenic Ras simultaneously activates several downstream molecules including Raf, PI3-K, and p38 MAPK. The Raf/MEK/ERK pathway mainly transduces proliferation and survival signals, while the remaining pathways commonly induce growth arrest (senescence) through cell cycle regulatory molecules such as p16^{INK4a}, p19^{ARF}, p21$^{CIP1/WAF1}$, and p53. So, oncogenic Ras is supposed to induce proliferation or senescence dependently on the balance between these two signals. In this study, we found that GATA-1 inhibits mitogenic signal from Ras through its interaction with MEK1 in erythroid cells, which resulted in their growth inhibition due to the dominance of senescence-inducing signals. In addition, we found that p21$^{CIP1/WAF1}$ is a crucial regulator of oncogenic Ras-induced senescence of erythroid cells.

as Jun N-terminal kinase (JNK) and protein kinase C (PKC) in CML cells (49). Alternatively, it is also possible that the interaction between GATA-1 and MEK might be inhibited in megakaryocytes due to the presence of some nuclear protein(s) specific for this lineage. However, further studies are required to clarify how megakaryocytes develop and platelets are effectively produced in CML patients.

Among various signaling molecules downstream of Ras, the Raf/MEK/ERK pathway mainly promotes cell growth and prevents apoptosis of hematopoietic cells (14). On the other hand, oncogenic stimuli including constitutively activated Ras, also cause growth inhibition (senescence) that acts as a fail-safe mechanism against malignant transformation (15, 16, 21). Although the mechanism of Ras-induced senescence is not fully understood, recent findings have unveiled several MEK/ERK-independent pathways (19). These pathways regulate the function of two main tumor-suppressor molecules, p53 and retinoblastoma protein (pRb) (50). Downstream of oncogenic Ras, p38-regulated/activated protein kinase (PRAK), a substrate of p38 mitogen-activated protein kinase (p38 MAPK), activates p53 by direct phosphorylation (20). Ras/Raf stabilizes p53 independently of MEK through the up-regulation of p19^{ARF} (21). The PI3-K pathway also stabilizes p53 through the inhibition of H/MDM2 (19). So, we speculated that N-RasE12 might induce growth arrest in erythroid cells even if MEK activities are blocked by GATA-1.

Ras-induced senescence is executed by CDK inhibitors such as p16^{INK4a} and p21$^{CIP1/WAF1}$, and a tumor-suppressor, p19^{ARF}, which consequently activate both p53 and pRb pathways. Among these molecules, we here found that p21$^{CIP1/WAF1}$ is a major player of Ras-induced suppression of erythropoiesis (may well be called nearly equal to senescence). Although p21$^{CIP1/WAF1}$ is a transcriptional target of p53 (51), p53 deficiency did not cancel Ras-induced suppression of erythropoiesis. So, p53-independent expression of p21$^{CIP1/WAF1}$ was supposed to be important for Ras-induced suppression of erythropoiesis. Because Darley *et al.* (18) previously showed that oncogenic N-Ras conferred developmental abnormalities on human erythroid cells through the activation of PKC, one of the reported activators of p21$^{CIP1/WAF1}$ (52), PKC may be a candidate molecule involved in Ras-induced expression of p21$^{CIP1/WAF1}$ and consequent suppression of erythropoiesis.

Mutation and/or deletion of the p53 gene and the INK4a/ARF locus are frequently observed in CML blast phase (1), but to our knowledge, there is no report demonstrating the inactivation of the p21$^{CIP1/WAF1}$ gene. So, our findings that p21$^{CIP1/WAF1}$ but not p53 or p16^{INK4a}/p19^{ARF} is the major regulator of Ras-induced suppression of erythropoiesis are again consistent with the clinical features that anemia is continued and erythroid transformation is a rare event in blast-phase

Downloaded from www.jbc.org at OSAKA UNIVERSITY, on May 12, 2011

CML (7, 8). Furthermore, because loss-of-function mutations of the p21$^{CIP1/WAF1}$ gene are rare in most of the hematologic malignancies, anemia observed in these diseases might be attributable to p21$^{CIP1/WAF1}$.

In conclusion, we here show that BCR-ABL but not JAK2 V617F inhibits erythropoiesis through the Ras signal. We also identified p21$^{CIP1/WAF1}$ as a central regulator of Ras-induced suppression of erythropoiesis. Ras transmits both growth promoting and inhibitory signals, and then induces proliferation or senescence dependently on their balance. In erythroid but not in myeloid progenitors, the growth promoting signal is inhibited at the level of MEK by GATA-1, which would lead to the relative dominance of the growth inhibitory signal mediated by p21$^{CIP1/WAF1}$ (Fig. 7). These mechanisms would explain why oncogenic Ras simultaneously reveals conflicting effects according to the cell lineage, *i.e.* growth promotion in myeloid cells and growth inhibition in erythroid cells. This model may be also useful to understand the mechanism of anemia caused by other oncogenic TKs.

Acknowledgments—We thank Dr. Connie J. Eaves for providing the vector expressing p210-BCR-ABL, Dr. Kazuya Shimoda for providing the plasmid encoding JAK2 V617F, and Dr. Hiroyuki Miyoshi for providing 293gp cells.

REFERENCES

1. Quintás-Cardama, A., and Cortes, J. (2009) *Blood* **113,** 1619–1630
2. Small, D. (2006) *Hematology Am. Soc. Hematol. Educ. Program,* 178–184
3. Levine, R. L., and Gilliland, D. G. (2008) *Blood* **112,** 2190–2198
4. Ren, R. (2005) *Nat. Rev. Cancer* **5,** 172–183
5. Zeuner, A., Pedini, F., Signore, M., Ruscio, G., Messina, C., Tafuri, A., Girelli, G., Peschle, C., and De Maria, R. (2006) *Blood* **107,** 3495–3502
6. Thiele, J., Kvasnicka, H. M., Schmitt-Graeff, A., Zirbes, T. K., Birnbaum, F., Kressmann, C., Melguizo-Grahmann, M., Frackenpohl, H., Sprungmann, C., Leder, L. D., Diehl, V., Zankovich, R., Schaefer, H. E., Niederle, N., and Fischer, R. (2000) *Leuk. Lymphoma* **36,** 295–308
7. Saikia, T., Advani, S., Dasgupta, A., Ramakrishnan, G., Nair, C., Gladstone, B., Kumar, M. S., Badrinath, Y., and Dhond, S. (1988) *Leuk. Res.* **12,** 499–506
8. Griffin, J. D., Todd, R. F., 3rd, Ritz, J., Nadler, L. M., Canellos, G. P., Rosenthal, D., Gallivan, M., Beveridge, R. P., Weinstein, H., Karp, D., and Schlossman, S. F. (1983) *Blood* **61,** 85–91
9. Sonoyama, J., Matsumura, I., Ezoe, S., Satoh, Y., Zhang, X., Kataoka, Y., Takai, E., Mizuki, M., Machii, T., Wakao, H., and Kanakura, Y. (2002) *J. Biol. Chem.* **277,** 8076–8082
10. Sexl, V., Piekorz, R., Moriggl, R., Rohrer, J., Brown, M. P., Bunting, K. D., Rothammer, K., Roussel, M. F., and Ihle, J. N. (2000) *Blood* **96,** 2277–2283
11. Hoelbl, A., Kovacic, B., Kerenyi, M. A., Simma, O., Warsch, W., Cui, Y., Beug, H., Hennighausen, L., Moriggl, R., and Sexl, V. (2006) *Blood* **107,** 4898–4906
12. Sawyers, C. L., McLaughlin, J., and Witte, O. N. (1995) *J. Exp. Med.* **181,** 307–313
13. Baum, K. J., and Ren, R. (2008) *J. Hematol. Oncol.* **1,** 5
14. Platanias, L. C. (2003) *Blood* **101,** 4667–4679
15. Campisi, J. (2005) *Cell* **120,** 513–522
16. Braig, M., and Schmitt, C. A. (2006) *Cancer Res.* **66,** 2881–2884
17. Darley, R. L., Hoy, T. G., Baines, P., Padua, R. A., and Burnett, A. K. (1997) *J. Exp. Med.* **185,** 1337–1347
18. Darley, R. L., Pearn, L., Omidvar, N., Sweeney, M., Fisher, J., Phillips, S., Hoy, T., and Burnett, A. K. (2002) *Blood* **100,** 4185–4192
19. Yaswen, P., and Campisi, J. (2007) *Cell* **128,** 233–234
20. Sun, P., Yoshizuka, N., New, L., Moser, B. A., Li, Y., Liao, R., Xie, C., Chen, J., Deng, Q., Yamout, M., Dong, M. Q., Frangou, C. G., Yates, J. R., 3rd, Wright, P. E., and Han, J. (2007) *Cell* **128,** 295–308
21. Wahl, G. M., and Carr, A. M. (2001) *Nat. Cell Biol.* **3,** E277–286
22. Ezoe, S., Matsumura, I., Gale, K., Satoh, Y., Ishikawa, J., Mizuki, M., Takahashi, S., Minegishi, N., Nakajima, K., Yamamoto, M., Enver, T., and Kanakura, Y. (2005) *J. Biol. Chem.* **280,** 13163–13170
23. Delgado, M. D., Vaqué, J. P., Arozarena, I., López-Ilasaca, M. A., Martínez, C., Crespo, P., and León, J. (2000) *Oncogene* **19,** 783–790
24. Onishi, M., Nosaka, T., Misawa, K., Mui, A. L., Gorman, D., McMahon, M., Miyajima, A., and Kitamura, T. (1998) *Mol. Cell. Biol.* **18,** 3871–3879
25. Egawa, K., Sharma, P. M., Nakashima, N., Huang, Y., Huver, E., Boss, G. R., and Olefsky, J. M. (1999) *J. Biol. Chem.* **274,** 14306–14314
26. Jiang, X., Ng, E., Yip, C., Eisterer, W., Chalandon, Y., Stuible, M., Eaves, A., and Eaves, C. J. (2002) *Blood* **100,** 3731–3740
27. Shide, K., Shimoda, H. K., Kumano, T., Karube, K., Kameda, T., Takenaka, K., Oku, S., Abe, H., Katayose, K. S., Kubuki, Y., Kusumoto, K., Hasuike, S., Tahara, Y., Nagata, K., Matsuda, T., Ohshima, K., Harada, M., and Shimoda, K. (2008) *Leukemia* **22,** 87–95
28. Matsumura, I., Kanakura, Y., Kato, T., Ikeda, H., Horikawa, Y., Ishikawa, J., Kitayama, H., Nishiura, T., Tomiyama, Y., Miyazaki, H., and Matsuzawa, Y. (1996) *Blood* **88,** 3074–3082
29. Fukushima, K., Matsumura, I., Ezoe, S., Tokunaga, M., Yasumi, M., Satoh, Y., Shibayama, H., Tanaka, H., Iwama, A., and Kanakura, Y. (2009) *J. Biol. Chem.* **284,** 7719–7732
30. Roussel, M. F. (1999) *Oncogene* **18,** 5311–5317
31. el-Deiry, W. S., Tokino, T., Velculescu, V. E., Levy, D. B., Parsons, R., Trent, J. M., Lin, D., Mercer, W. E., Kinzler, K. W., and Vogelstein, B. (1993) *Cell* **75,** 817–825
32. Macleod, K. F., Sherry, N., Hannon, G., Beach, D., Tokino, T., Kinzler, K., Vogelstein, B., and Jacks, T. (1995) *Genes Dev.* **9,** 935–944
33. Parker, S. B., Eichele, G., Zhang, P., Rawls, A., Sands, A. T., Bradley, A., Olson, E. N., Harper, J. W., and Elledge, S. J. (1995) *Science* **267,** 1024–1027
34. Khalaf, W. F., White, H., Wenning, M. J., Orazi, A., Kapur, R., and Ingram, D. A. (2005) *Blood* **105,** 3538–3541
35. Sui, X., Krantz, S. B., You, M., and Zhao, Z. (1998) *Blood* **92,** 1142–1149
36. Esteban, L. M., Vicario-Abejón, C., Fernández-Salguero, P., Fernández-Medarde, A., Swaminathan, N., Yienger, K., Lopez, E., Malumbres, M., McKay, R., Ward, J. M., Pellicer, A., and Santos, E. (2001) *Mol. Cell. Biol.* **21,** 1444–1452
37. Umanoff, H., Edelmann, W., Pellicer, A., and Kucherlapati, R. (1995) *Proc. Natl. Acad. Sci. U.S.A.* **92,** 1709–1713
38. Zhang, J., Socolovsky, M., Gross, A. W., and Lodish, H. F. (2003) *Blood* **102,** 3938–3946
39. MacKenzie, K. L., Dolnikov, A., Millington, M., Shounan, Y., and Symonds, G. (1999) *Blood* **93,** 2043–2056
40. Metcalfe, D. D. (2008) *Blood* **112,** 946–956
41. Wheadon, H., and Welham, M. J. (2003) *Blood* **102,** 1480–1489
42. Döhner, K., and Döhner, H. (2008) *Haematologica* **93,** 976–982
43. Neubauer, A., Greenberg, P., Negrin, R., Ginzton, N., and Liu, E. (1994) *Leukemia* **8,** 638–641
44. Flotho, C., Valcamonica, S., Mach-Pascual, S., Schmahl, G., Corral, L., Ritterbach, J., Hasle, H., Aricò, M., Biondi, A., and Niemeyer, C. M. (1999) *Leukemia* **13,** 32–37
45. Akashi, K., Traver, D., Miyamoto, T., and Weissman, I. L. (2000) *Nature* **404,** 193–197
46. Zhang, J., Liu, Y., Beard, C., Tuveson, D. A., Jaenisch, R., Jacks, T. E., and Lodish, H. F. (2007) *Blood* **109,** 5238–5241
47. Lenormand, P., Sardet, C., Pagès, G., L'Allemain, G., Brunet, A., and Pouysségur, J. (1993) *J. Cell Biol.* **122,** 1079–1088
48. Jaaro, H., Rubinfeld, H., Hanoch, T., and Seger, R. (1997) *Proc. Natl. Acad. Sci. U.S.A.* **94,** 3742–3747
49. Jacquel, A., Herrant, M., Defamie, V., Belhacene, N., Colosetti, P., Marchetti, S., Legros, L., Deckert, M., Mari, B., Cassuto, J. P., Hofman, P., and Auberger, P. (2006) *Oncogene* **25,** 781–794
50. Serrano, M., Lin, A. W., McCurrach, M. E., Beach, D., and Lowe, S. W. (1997) *Cell* **88,** 593–602
51. Deng, Y., Chan, S. S., and Chang, S. (2008) *Nat. Rev. Cancer* **8,** 450–458
52. Biggs, J. R., Kudlow, J. E., and Kraft, A. S. (1996) *J. Biol. Chem.* **271,** 901–906

Downloaded from www.jbc.org at OSAKA UNIVERSITY, on May 12, 2011

Int J Hematol (2010) 92:111–117
DOI 10.1007/s12185-010-0621-x

ORIGINAL ARTICLE

Imatinib for newly diagnosed chronic-phase chronic myeloid leukemia: results of a prospective study in Japan

Tadashi Nagai · Jin Takeuchi · Nobuaki Dobashi · Yuzuru Kanakura · Shuichi Taniguchi · Koji Ezaki · Chiaki Nakaseko · Akira Hiraoka · Masaya Okada · Yasushi Miyazaki · Toshiko Motoji · Masaaki Higashihara · Norifumi Tsukamoto · Hitoshi Kiyoi · Shinji Nakao · Katsuji Shinagawa · Ryuzo Ohno · Tomoki Naoe · Kazunori Ohnishi · Noriko Usui

Received: 22 December 2009 / Revised: 7 May 2010 / Accepted: 31 May 2010 / Published online: 25 June 2010
© The Japanese Society of Hematology 2010

Abstract Although imatinib has become the current standard treatment for chronic myeloid leukemia (CML), there is limited information regarding its efficacy and safety among Japanese patients. We therefore conducted a prospective multi-center open-label study of imatinib for Japanese patients with newly diagnosed chronic-phase CML (CP-CML). A total of 107 patients were enrolled and treated with imatinib at an initial daily dose of 400 mg. Eighty-three patients completed 3 years of study treatment. The cumulative rates of major cytogenetic response and complete cytogenetic response (CCyR) were 90.9 and 90.2% at 3 years, respectively. The safety profile was not very different from that reported in the IRIS study, although grade ≥3 neutropenia occurred relatively frequently (31.8 vs. 14.3%). Only seven patients discontinued the study due to adverse events, as did four patients due to

T. Nagai and J. Takeuchi contributed equally to this study, and the order in which they are listed should be considered arbitrary.

T. Nagai (✉)
Division of Hematology, Jichi Medical University Hospital, Shimotsuke 329-0498, Japan
e-mail: t-nagai@jichi.ac.jp

J. Takeuchi
Nihon University Itabashi Hospital, Tokyo, Japan

N. Dobashi · N. Usui
Jikei University Hospital, Tokyo, Japan

Y. Kanakura
Osaka University Hospital, Osaka, Japan

S. Taniguchi
Toranomon Hospital, Tokyo, Japan

K. Ezaki
Fujita Health University Hospital, Toyoake, Japan

C. Nakaseko
Chiba University Hospital, Chiba, Japan

A. Hiraoka
Osaka Medical Center for Cancer and Cardiovascular Diseases, Osaka, Japan

M. Okada
The Hospital of Hyogo College of Medicine, Hyogo, Japan

Y. Miyazaki
Nagasaki University Hospital, Nagasaki, Japan

T. Motoji
Tokyo Women's Medical University, Tokyo, Japan

M. Higashihara
Kitasato University Hospital, Sagamihara, Japan

N. Tsukamoto
Gunma University Hospital, Maebashi, Japan

H. Kiyoi · T. Naoe
Nagoya University Hospital, Nagoya, Japan

S. Nakao
Kanazawa University Hospital, Kanazawa, Japan

K. Shinagawa
Okayama University Hospital, Okayama, Japan

R. Ohno
Aichi Cancer Center, Nagoya, Japan

K. Ohnishi
Hamamatsu University School of Medicine, Hamamatsu, Japan

insufficient efficacy. The 3-year probabilities of overall survival and progression-free survival were 93.2 and 91.4%, respectively. Higher average daily doses (i.e., ≥350 mg) were significantly associated not only with higher rates of achieving CCyR, but also with longer duration of CCyR. These findings confirm the clinical utility of imatinib in Japanese patients with newly diagnosed CP-CML, and suggest detrimental effect of low average daily dose on treatment results.

Keywords Chronic myeloid leukemia · Chronic phase · Newly diagnosed · Imatinib

1 Introduction

Imatinib is a molecule-targeting drug that inhibits BCR-ABL tyrosine kinase and exerts a selective proliferation-inhibitory effect in chronic myeloid leukemia (CML) [1, 2]. Several international trials have documented excellent clinical efficacy of imatinib in patients with chronic-phase CML (CP-CML) [3–5], as well as in patients in accelerated phase (AP) [6] and blast crisis (BC) [7]. Based on those studies along with Japanese phase I and phase II studies [8], imatinib was approved in Japan in November 2001, and has been available in clinical practice since December 2001. However, there is very limited information regarding efficacy and safety of imatinib among Japanese patients. We therefore conducted a post-marketing study to confirm clinical utility of imatinib in Japanese patients with newly diagnosed CP-CML.

2 Patients and methods

2.1 Study design

This was a prospective, multi-center, non-controlled study to evaluate efficacy and safety of imatinib in Japanese patients 15–74 years of age with Philadelphia chromosome positive (Ph+) CP-CML. Eligible patients were those with Eastern Cooperative Oncology Group performance status 0–3 who had been previously untreated with interferon (IFN) or imatinib. Patients were excluded if serum bilirubin or serum creatinine levels were ≥3 times the upper limit of the normal range, if serum aspartate aminotransferase (AST) or alanine aminotransferase (ALT) levels were ≥5 times the upper limit of the normal range, if they received hydroxycarbamide within a week prior to enrollment or any other antileukemic drug within 2 weeks, or if there was any evidence of AP or BC in association with any of the following conditions: ≥15% blasts in the peripheral blood or bone marrow; ≥30% blasts plus promyelocytes in the peripheral blood or bone marrow; ≥20% basophils in the peripheral blood; or extramedullary leukemic infiltrates with the exception of spleen or liver. Women who were pregnant or possibly pregnant were also excluded.

Patients were treated with imatinib at a daily dose of 400 mg. Dose escalation to 600 mg was implemented if they had failed to achieve complete hematologic response (CHR) at 3 months or major cytogenetic response (MCyR) at 6 months. If the patient had failed to achieve MCyR at 9 months, IFN was started at a daily dose of 300 million unit per body two or three times a week while on imatinib. Dose modification of imatinib was generally based on the following guidelines. For grade ≥3 liver dysfunction (elevated bilirubin, AST, or ALT), administration was interrupted until recovery to grade <2, and then resumed at 300 mg/day. For grade ≥3 neutropenia or thrombocytopenia, administration was interrupted until recovery to grade <2, and then resumed at 400 mg/day. If grade ≥3 toxicity recurred after resuming, dose reduction to 300 mg/day was implemented. The study was discontinued in the event of failure to achieve CHR at 6 months, intolerance to imatinib, disease progression to AP or BC, death, patient request, and lost to follow-up, or at the discretion of the investigator. Patients were followed up to 3 years from the day of starting imatinib.

2.2 Endpoints

The primary endpoints were overall survival (OS) and progression-free survival (PFS). OS was defined as the time from the day of first dose of imatinib to death or last follow-up, and PFS was defined as the time from the day of first dose of imatinib to progression to AP or BC, death or last follow-up. Secondary endpoints were hematologic, cytogenetic and molecular response, and adverse events. Cytogenetic response was assessed by using bone marrow cells every 3 months until 12 months and every 6 months thereafter until 36 months. Complete cytogenetic response (CCyR) was defined as complete disappearance of the Philadelphia chromosome. MCyR was defined as decrease in Philadelphia chromosome to 35% or lower. Adverse events were assessed according to the National Cancer Institute Common Toxicity Criteria version 2.0.

Cumulative rates of hematologic and cytogenetic response, PFS, event-free survival (EFS), and OS were evaluated in accordance with the IRIS study reports [3, 9]. EFS was defined as the time from the day of first dose of imatinib to death, progression to AP or BC, loss of CHR, loss of MCyR, increase in white blood cell count to 20000/μL, or last follow-up.

This study was conducted in compliance with the Declaration of Helsinki and was approved by local Institutional Review Boards. All patients provided written informed consent prior to initiation of study medication.

2.3 Statistical methods

OS, PFS, and EFS were estimated by using the Kaplan–Meier method. Efficacy endpoints were compared by patient age (≥60 years and <60 years), and by average daily dose of imatinib (i.e., ≥350 mg/day, 250 to <350 mg/day and <250 mg/day). The Wilcoxon two-sample test was used to compare the average daily dose between the age groups. In patients who had achieved CCyR, CCyR duration was compared by average daily dose of imatinib after achieving CCyR. Average daily dose was calculated as cumulative dosage divided by the total days on study.

3 Results

3.1 Patients

A total of 107 patients were enrolled in the study between November 2002 and June 2004, and administered imatinib. All patients were evaluable for efficacy and safety, and the median duration of imatinib exposure was 1091 days (range, 82–1156 days). Among these patients, 83 completed 3 years of study treatment, whereas 24 discontinued the study due to adverse events ($n = 7$), withdrawal of consent ($n = 5$), insufficient efficacy ($n = 4$), allogeneic bone marrow transplantation ($n = 4$), and other reasons ($n = 4$). Demographic characteristics of patients in the full analysis set are summarized in Table 1. The median age was 47 years (range, 16–74 years), with 71 males and 36 females. Prior therapies for CML included hydroxycarbamide ($n = 7$), and leukapheresis ($n = 1$). The median time from diagnosis of CML to initiation of imatinib was 8.0 days (range, 1–1526 days).

The initial dose of imatinib was 400 mg/day for all patients. The mean (±standard deviation) dose administered during the study was 343 (±90) mg/day. Dose modification was required in 70.1% of patients mainly due to adverse events. Details of dose modification are summarized in Table 2. There were no patients in whom IFN was added to imatinib. Average daily doses were ≥350 mg, 250 to <350 mg, and <250 mg in 68 (63.6%), 21 (19.6%) and 18 patients (16.8%), respectively. As shown in Table 3, the percentage of patients who continued imatinib at 400 mg/day without any dose modification was 48.6% during week 1–13, 57.5% during week 14–26, and was around 60% thereafter.

3.2 Treatment results

The cumulative rate of CHR was 99.1% at 1 year, and the cumulative rates of MCyR and CCyR were 90.9 and 90.2% at 3 years, respectively (Fig. 1). The median time to CHR

Table 1 Patient characteristics

Characteristics	Category	Number of patients
Total number of subjects		107
Sex	Male	71 (66.4)
	Female	36 (33.6)
Age	10s	4 (3.7)
	20s	10 (9.3)
	30s	24 (22.4)
	40s	18 (16.8)
	50s	26 (24.3)
	60s	19 (17.8)
	70s	6 (5.6)
	Mean ± SD	47.1 ± 14.7
	Minimum–maximum	16–74
	Median	47.0
Body weight	40 to <50 kg	13 (12.1)
	50 to <60 kg	34 (31.8)
	60 to <70 kg	40 (37.4)
	70 to <80 kg	13 (12.1)
	80 to <90 kg	5 (4.7)
	≥90 kg	2 (1.9)
	Mean ± SD	61.66 ± 10.88
	Minimum–maximum	43.0–103.0
	Median	61.50
Body surface area	1.2 to <1.4 m^2	5 (4.7)
	1.4 to <1.6 m^2	31 (29.0)
	1.6 to <1.8 m^2	53 (49.5)
	1.8 to <2.0 m^2	15 (14.0)
	≥2.0 m^2	3 (2.8)
	Mean ± SD	1.6705 ± 0.1670
	Minimum–maximum	1.307–2.151
	Median	1.6800
Previous CML therapy	No	99 (92.5)
	Yes	8 (7.5)
	Hydroxycarbamide	7 (6.5)
	Leukapheresis	1 (0.9)
ECOG performance status	0	95 (88.8)
	1	10 (9.3)
	2	2 (1.9)
Time elapsed from the first day of CML diagnosis to the start of study treatment	<4 weeks	92 (86.0)
	4 to <13 weeks	14 (13.1)
	≥52 weeks	1 (0.9)
	Mean ± SD	27.0 ± 146.9
	Minimum–maximum	1–1526
	Median	8.0

Values within parenthesis are given in percentage

SD standard deviation, *CML* chronic myeloid leukemia, *ECOG* Eastern Cooperative Oncology Group

and CCyR were 92.5 days (range, 75–207 days) and 179.5 days (range, 70–589 days), respectively. In 92 patients who had achieved CCyR, 77 patients remained in CCyR until the end of 3 years of imatinib treatment. All of the 15 patients who hadn't achieved CCyR discontinued the study. Among them, 4 patients progressed to AP or BC, and 5 patients proceeded to hematopoietic stem cell transplantation.

Of 107 patients, progression to AP or BC and death occurred in nine and seven patients, respectively. One death, which was because of pneumonia, was reported during the study and the remaining six deaths were reported after patients discontinued the study. The probabilities of OS, PFS and EFS at 3 years were 93.2% [95% confidence interval (CI) 88.3–98.1%), 91.4% (95% CI 86.1–96.8%), and 81.9% (95% CI 74.6–89.3%), respectively (Fig. 2).

3.3 Response and survival by average daily dose

Next, we evaluated cumulative CCyR rate, OS, PFS, and EFS according to the average daily dose of imatinib (≥350 mg/day, 250 to <350 mg/day, and <250 mg/day). As shown in Figs. 3, 4, CCyR and EFS were significantly associated with the average daily dose ($p < 0.001$, respectively). In particular, patients with the average daily dose <250 mg had low rates of CCyR and EFS. CCyR duration was also significantly different according to the average daily dose ($p < 0.001$, Fig. 5). OS and PFS seemed lower in those with lower average daily dose, although the differences did not reach statistical significance.

The average daily doses were significantly different by age group, with 360 (±81) mg in patients aged <60, and 287 (±97) mg in patients aged ≥60 years ($p < 0.001$). Patients aged <60 had statistically non-significant better EFS than those aged ≥60 years (85.3 vs. 70.6% at 3 years, $p = 0.101$). In terms of OS or PFS, there were no significant differences between the age groups.

Table 2 Summary of dose modification

	n	%
No dose change	32	29.9
Dose change	75	70.1
Reduction only	7	6.5
Reduction and interruption	43	40.2
Reduction and increase	1	0.9
Increase only	1	0.9
Increase and interruption	4	3.7
Interruption only	19	17.8
Total	107	100.0

3.4 Adverse events

Adverse events were reported in all of the 107 patients. Serious adverse events which developed in ≥2 patients included neutropenia ($n = 4$), blast crisis ($n = 3$), anemia, intestinal obstruction, gastric antral vascular ectasia, appendicitis, herpes zoster, thrombocytopenia, and leukocytopenia ($n = 2$, each). Grade ≥3 adverse events were reported in 31 patients (29.0%, 47 episodes). As listed in Table 4, grade ≥3 adverse events reported in >5% of patients were neutropenia (31.8%), leukocytopenia (19.6%), lymphocytopenia (17.8%), thrombocytopenia (14.0%), and rash (8.4%). When frequencies of adverse events were compared between this study and the IRIS study [3], nasopharyngitis, rash, upper respiratory tract infection, pyrexia, and grade ≥3 neutropenia seemed more frequent, while nausea, muscle cramp, joint pain seemed less frequent in our study.

4 Discussion

Although it is widely accepted that imatinib is the standard treatment for CP-CML, published experiences of imatinib

Table 3 Average daily dose of imatinib over time

Week:	1–13		14–26		27–39		40–52		53–78		79–104		105–130		131–156	
No. of patients (*n*):	107		106		102		95		92		90		88		88	
Average daily dose (mg)	*n*	%	*n*	%	*n*	%	*n*	%	*n*	%	*n*	%	*n*	%	*n*	%
<200	3	2.8	12	11.3	9	8.8	7	7.4	6	6.5	4	4.4	3	3.4	1	1.1
200 to <300	24	22.4	16	15.1	11	10.8	7	7.4	9	9.8	9	10.0	9	10.2	14	15.9
300 to <350	13	12.1	12	11.3	14	13.7	18	18.9	12	13.0	12	13.3	16	18.2	12	13.6
350 to <400	15	14.0	4	3.8	4	3.9	0	0.0	5	5.4	5	5.6	4	4.5	6	6.8
400	52	48.6	61	57.5	61	59.8	61	64.2	58	63.0	58	64.4	54	61.4	52	59.1
>400	0	0.0	1	0.9	3	2.9	2	2.1	2	2.2	2	2.2	2	2.3	3	3.4

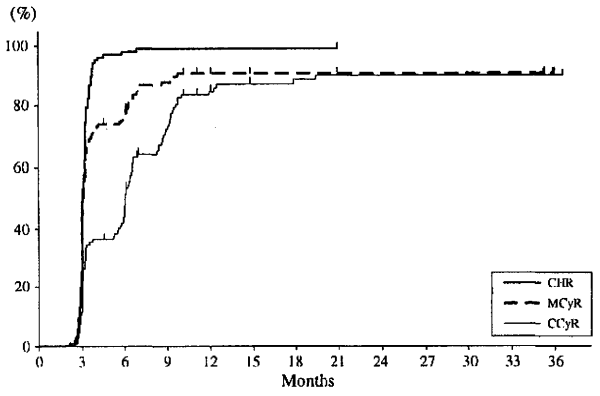

Fig. 1 Kaplan–Meier curves of cumulative rates of complete hematologic response (*CHR*), major cytogenetic response (*MCyR*) and complete cytogenetic response (*CCyR*)

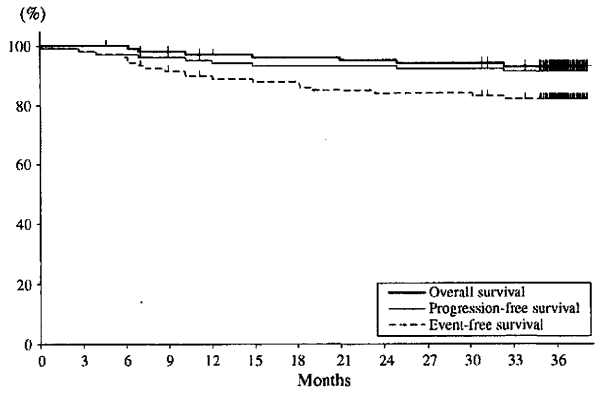

	No. of Events	Estimated 3-year rate (%)
OS	7	93.2
PFS	9	91.4
EFS	19	81.9

Fig. 2 Kaplan–Meier curves of overall survival, progression-free survival and event-free survival of all patients

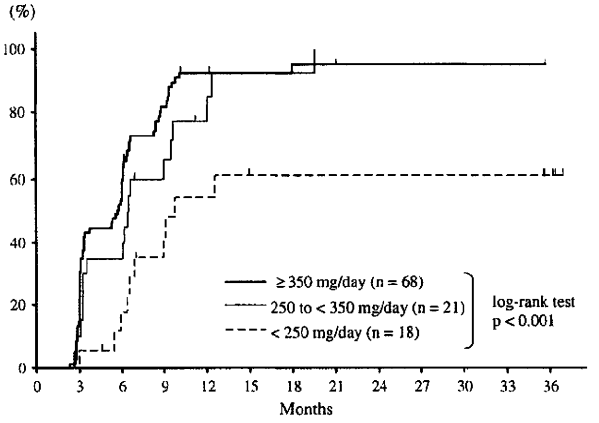

Fig. 3 Kaplan–Meier curves of cumulative rates of complete cytogenetic response (CCyR) by average daily dose of imatinib

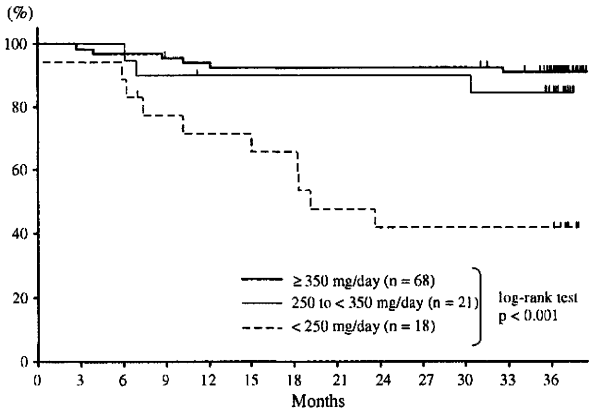

Fig. 4 Kaplan–Meier curves of event-free survival by average daily dose of imatinib

in Japanese patients are limited [8, 10–16]. Under such circumstances, a nationwide registration system for CML has been established by the Japanese Society of Hematology since 2003, and early results were published [15]. To further clarify the clinical utility of imatinib among Japanese patients, we conducted a prospective study of imatinib in 109 patients with newly diagnosed CP-CML. MCyR and CCyR rates at 12 months were 90.9 and 84.8%, which were comparable or even superior to those in the IRIS study (85 and 69%, respectively) [9]. Likewise, long-term outcomes were not different between both studies, because the OS rate in our study was 93.2% at 3 years, whereas, in the IRIS study, it was reported to be 97.2% at 18 months and 89% at 5 years [3, 9]. The safety profile observed in our study was almost comparable with that of the IRIS study, although grade ≥3 neutropenia occurred relatively frequently in our study than in the IRIS study (31.8 vs. 14.3%), while the incidences of neutropenia of all grades were not different (53.3% in our study versus 60.8% in the IRIS study). In both studies, imatinib was initiated at a daily dose of 400 mg and interrupted in the event of grade ≥3 neutropenia or thrombocytopenia until the toxicity resolved to grade <2. The reason for this observation was not clear; however, the finding that only seven of our patients discontinued the study due to adverse events showed feasibility of the treatment. Some non-hematological adverse events like nausea, muscle cramp, and joint pain were less frequent in Japanese than in Caucasians. These efficacy and safety results, taken together, confirmed the clinical utility of imatinib in Japanese patients with newly diagnosed CP-CML.

Based upon observations in a relatively small number of Japanese patients, some authors have suggested the possibility that the daily dose of imatinib could be reduced to less than 400 mg without significant disadvantage, partly

due to smaller body size as compared with Caucasians [12, 13]. Analyses of cumulative rate of CCyR and EFS by average daily dose in our study showed that patients given higher average daily doses of imatinib (≥350 mg) not only achieved higher CCyR rate but also had longer CCyR duration than those given lower average daily doses. EFS was also superior among patients who were treated with higher average daily doses of imatinib. Matsuo et al. [10] reported similar findings of a clear dose–response relationship between imatinib daily dose and treatment results. In that study, CCyR rate at 30 months was higher in patients receiving daily dose of imatinib >300 mg than in those receiving 250–300 mg, or <250 mg. Sugita et al. [16] also reported that mean daily doses of ≥300 mg led to higher CCyR rate, longer CCyR duration, and improved OS as compared to 200–300 mg. These results, taken together, suggest detrimental effect of low average daily dose on treatment results. Our observation that EFS was relatively lower in patients aged ≥60 years than in those aged <60 years might be explained partly by the difference in the average daily dose. To achieve and maintain better response, it would be beneficial to avoid excessive dose

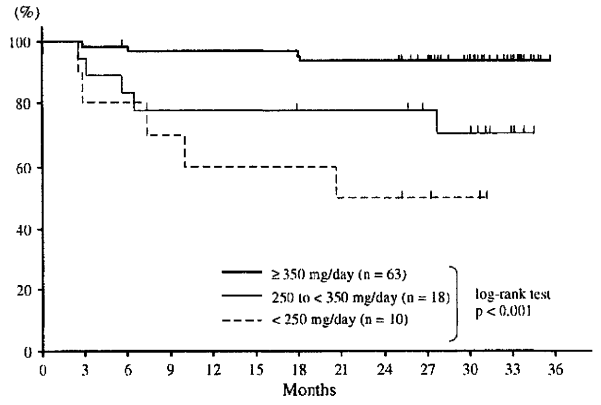

Fig. 5 Kaplan–Meier curves of duration of complete cytogenetic response (CCyR)

Table 4 Comparison of adverse events between this study and the IRIS study

	This study (n = 107)				IRIS study (n = 533) [3]			
	All grades		Grade 3/4		All grades		Grade 3/4	
	n	%	n	%	n	%	n	%
Hematological								
Neutropenia	57	53.3	34	31.8	324	60.8	76	14.3
Leukocytopenia	51	47.7	21	19.6	NR	NR	NR	NR
Lymphocytopenia	48	44.9	19	17.8	NR	NR	NR	NR
Thrombocytopenia	44	41.1	15	14.0	302	56.6	42	7.8
Anemia	33	30.8	3	2.8	238	44.6	17	3.1
Nonhematological								
Surficial edema	71	66.4	0	0.0	296	55.5	5	0.9
Nasopharyngitis	70	65.4	0	0.0	117	22.0	0	0.0
Rash	64	59.8	9	8.4	181	33.9	11	2.0
Diarrhea	44	41.1	3	2.8	175	32.8	10	1.8
Gastroenteritis	37	34.6	3	2.8	NR	NR	NR	NR
Nausea	35	32.7	0	0.0	233	43.7	4	0.7
Malaise	29	27.1	0	0.0	184	34.5	6	1.1
Myalgia	27	25.2	2	1.9	114	21.4	8	1.5
Upper respiratory tract infection	27	25.2	0	0.0	77	14.5	1	0.2
Muscle cramps	26	24.3	0	0.0	204	38.3	7	1.3
Pyrexia	26	24.3	0	0.0	70	13.1	4	0.7
Headache	23	21.5	0	0.0	166	31.2	2	0.4
Dizziness	17	15.9	0	0.0	77	14.5	5	0.9
Vomiting	16	15.0	0	0.0	90	16.9	8	1.5
Joint pain	14	13.1	0	0.0	151	28.3	13	2.4
Cough	13	12.1	0	0.0	77	14.5	1	0.2
Anorexia	11	10.3	0	0.0	28	5.3	0	0.0
Pruritus	11	10.3	0	0.0	39	7.3	1	0.2

NR not reported

reduction and interruption with careful monitoring of safety in individual patients. A similar concept was advocated by a study reported by Kanda et al. [14].

In summary, this prospective study confirmed remarkable efficacy and safety of imatinib in Japanese patients with newly diagnosed CP-CML. It also suggested a clear relationship between higher daily doses of imatinib (i.e., $\geq$350 mg) and better treatment results.

Acknowledgments This study was sponsored by Novartis Pharma K.K. Contributing Investigators: Junji Tanaka, Hokkaido University Hospital; Koumei Kubo, Aomori Prefecture Central Hospital; Shuichi Taniguchi, Toranomon Hospital; Nobuaki Dobashi, Jikei University Hospital; Yasushi Isobe, Juntendo University School of Medicine; Jin Takeuchi, Nihon University Itabashi Hospital; Toshiko Motoji, Tokyo Women's Medical University; Masaaki Higashihara, Kitasato University Hospital; Tadashi Nagai, Jichi Medical University Hospital; Norifumi Tsukamoto, Gunma University Hospital; Chiaki Nakaseko, Chiba University Hospital; Kazuhiro Nishii, Mie University Hospital; Kazunori Ohnishi, Hamamatsu University School of Medicine, University Hospital; Yasuo Morishima, Aichi Cancer Center Hospital; Hitoshi Kiyoi, Nagoya University Hospital; Koji Ezaki, Fujita Health University; Yuzuru Kanakura, Osaka University Hospital; Akira Hiraoka, Osaka Medical Center for Cancer and Cardiovascular Diseases; Chihiro Shimazaki, University Hospital, Kyoto Prefectural University of Medicine; Masaya Okada, the Hospital of Hyogo College of Medicine; Shinji Nakao, Kanazawa University Hospital; Katsuji Shinagawa, Okayama University Hospital; Yasushi Miyazaki, Nagasaki University Hospital; Koji Nagafuji, Kyushu University Hospital.

References

1. Druker BJ, Tamura S, Buchdunger E, Ohno S, Segal GM, Fanning S, et al. Effects of a selective inhibitor of the Abl tyrosine kinase on the growth of Bcr-Abl positive cells. Nat Med. 1996;2:561–6.
2. Druker BJ, Talpaz M, Resta DJ, Peng B, Buchdunger E, Ford JM, et al. Efficacy and safety of a specific inhibitor of the BCR-ABL tyrosine kinase in chronic myeloid leukemia. N Eng J Med. 2001;344:1031–7.
3. O'Brien SG, Guilhot F, Larson RA, Gathmann I, Baccarani M, Cervantes F, et al. Imatinib compared with interferon and low-dose cytarabine for newly diagnosed chronic-phase chronic myeloid leukemia. N Eng J Med. 2003;348:994–1004.
4. Kantarjian H, Sawyers C, Hochhaus A, Guilhot F, Schiffer C, Gambacorti-Passerini C, et al. Hematologic and cytogenetic responses to imatinib mesylate in chronic myelogenous leukemia. N Eng J Med. 2002;346:645–52.
5. de Lavallade H, Apperley JF, Khorashad JS, Milojkovic D, Reid AG, Bua M, et al. Imatinib for newly diagnosed patients with chronic myeloid leukemia: incidence of sustained responses in an intention-to-treat analysis. J Clin Oncol. 2008;26:3358–63.
6. Talpaz M, Silver RT, Druker BJ, Goldman JM, Gambacorti-Passerini C, Guilhot F, et al. Imatinib induces durable hematologic and cytogenetic responses in patients with accelerated phase chronic myeloid leukemia: results of a phase 2 study. Blood. 2002;99:1928–37.
7. Sawyers CL, Hochhaus A, Feldman E, Goldman JM, Miller CB, Ottmann OG, et al. Imatinib induces hematologic and cytogenetic responses in patients with chronic myelogenous leukemia in myeloid blast crisis: results of a phase II study. Blood. 2002;99:3530–9.
8. Morishima Y, Ogura M, Nishimura M, Yazaki F, Bessho M, Mizoguchi H, et al. Efficacy and safety of imatinib mesylate for patients in the first chronic phase of chronic myeloid leukemia: results of a Japanese phase II clinical study. Int J Hematol. 2004;80(3):261–6.
9. Druker BJ, Guilhot F, O'Brien SG, Gathmann I, Kantarjian H, Gattermann N, et al. Five-year follow-up of patients receiving imatinib for chronic myeloid leukemia. N Eng J Med. 2006;355:2408–17.
10. Matsuo E, Miyazaki Y, Tsutsumi C, Inoue Y, Yamasaki R, Hata T, et al. Imatinib provides durable molecular and cytogenetic responses in a practical setting for both newly diagnosed and previously treated chronic myelogenous leukemia: a study in Nagasaki prefecture, Japan. Int J Hematol. 2007;85(2):132–9.
11. Ishikawa I, Kato C, Harigae H, Sugawara T, Tomiya Y, Yamada M, et al. Dose modification of imatinib by monitoring the level of BCR-ABL transcript in chronic myelogenous leukemia. Tohoku J Exp Med. 2006;210(4):355–63.
12. Horikoshi A, Takei K, Sawada S. Effects of lower doses of imatinib to CML patients. Leuk Res. 2003;27:1167.
13. Sakai M, Miyazaki Y, Matsuo E, Moriuchi Y, Hata T, Fukushima T, et al. Long-term efficacy of imatinib in a practical setting is correlated with imatinib trough concentration that is influenced by body size: a report by the Nagasaki CML Study Group. Int J Hematol. 2009;89(3):319–25.
14. Kanda Y, Okamoto S, Tauchi T, Kizaki M, Inokuchi K, Yabe M, et al. Multicenter prospective trial evaluating the tolerability of imatinib for Japanese patients with chronic myelogenous leukemia in the chronic phase: does body weight matter? Am J Hematol. 2008;83(11):835–9.
15. Kizaki M, Okamoto S, Tauchi T, Tanaka H, Tanimoto M, Inokuchi K, et al. Current and future perspectives on the TARGET system: the registration system for Glivec established by the JSH. Int J Hematol. 2008;88(4):409–17.
16. Sugita J, Tanaka J, Kurosawa M, Fukuhara T, Hashino S, Torimoto E, et al. Effects of the mean daily doses of imatinib during the first year on survival of patients with chronic myeloid leukemia in Japan: a study of the Hokkaido Hematology Study Group. Eur J Haematol. 2008;80(2):160–3.

Journal of Immunological Methods 359 (2010) 47–55

Contents lists available at ScienceDirect

Journal of Immunological Methods

journal homepage: www.elsevier.com/locate/jim

Research paper

Stromal cell-free conditions favorable for human B lymphopoiesis in culture

Michiko Ichii [a], Kenji Oritani [b], Takafumi Yokota [b], Daniel C. Schultz [c], Jennifer L. Holter [d], Yuzuru Kanakura [b], Paul W. Kincade [a,*]

[a] Immunobiology and Cancer Program, Oklahoma Medical Research Foundation, 825 NE13th Street, Oklahoma City, OK 73104, United States
[b] Department of Hematology and Oncology, Osaka University Graduate School of Medicine, Osaka, Japan
[c] Department of Obstetrics and Gynecology, University of Oklahoma Health Sciences Center, 920 Stanton L. Young, Oklahoma City, OK 73104, United States
[d] Department of Medicine, Hematology/Oncology, University of Oklahoma Health Sciences Center, 920 Stanton L. Young, Oklahoma City, OK 73104, United States

ARTICLE INFO

Article history:
Received 15 April 2010
Accepted 2 June 2010
Available online 9 June 2010

Keywords:
Human
B lymphopoiesis
G-CSF
Stromal cell-free cultures
Mesenchymal stem cell

ABSTRACT

Progress has been slow in defining molecular requirements for human B lymphopoiesis in part because of differences from experimental animals and also because of the lack of culture conditions that efficiently support the process. We recently found that human $CD10^+$ lymphocytes were produced when $CD34^+$ hematopoietic stem and progenitor cells were cultured in contact with human mesenchymal stem cells (hMSC). Further investigation revealed that it occurred even when progenitors were separated from hMSC by membrane filters. Experiments with neutralizing antibodies suggested that important heat labile factors produced by hMSC are unlikely to be IL-7, TSLP, CXCL12 or hemokinin-1. Further manipulation of culture conditions revealed that optimal lymphopoiesis required careful selection of fetal calf serum lots, maintenance of high cell densities, as well as recombinant cytokines (SCF, FL and G-CSF). G-CSF was particularly important when adult bone marrow rather than umbilical cord blood derived $CD34^+$ cells were used to initiate the cultures. These improved methods should facilitate identification of molecules that can be used to speed regeneration of the humoral immune system following chemotherapy and might suggest ways to inhibit growth of B lineage malignancies.

© 2010 Elsevier B.V. All rights reserved.

1. Introduction

B lineage lymphocytes are produced throughout life from hematopoietic stem cells (HSC) within bone marrow (BM) (Nunez et al., 1996; Rossi et al., 2003; Stephan et al., 1998). While steps in the process have been extensively investigated in mice, progress in understanding human B lymphopoiesis has been hampered by lack of efficient ways to study progenitors in culture (Bertrand et al., 2000; LeBien, 2000). This is partially due to species differences and a growth factor that selectively drives formation of human B cells has not been identified (Pribyl and LeBien, 1996). Some success has been obtained by placing human stem and progenitor cells on monolayers of murine stromal cells (Kurosaka et al., 1999; Nishihara et al., 1998;Ohkawara et al., 1998; Rawlings et al., 1995), and we recently found that human mesenchymal stem cells (hMSC) were even more effective (Ichii et al., 2008). For example, umbilical cord blood (CB) $CD34^+$ cells generated more $CD33^+$ $CD13^+$ myeloid cells and $CD10^+$ $CD19^+$ B lineage lymphocytes in hMSC co-cultures than when the murine MS5 stromal cell line was used. In addition to their support of hematopoiesis (Koç et al., 2000; Muguruma et al., 2006; Zhang et al., 2004), multipotential hMSC are capable of chondrocyte, osteoblast or adipocyte differentiation (Abdallah and Kassem, 2008; Chamberlain et al., 2007; Pittenger et al., 1999). Diffusible factors or membrane ligands on the adherent cells provide signals required for survival, proliferation and differentiation in the B lineage, but the nature of those molecules is poorly understood. Addition of recombinant growth and differentiation factors can be helpful, but optimal conditions have not been found.

Abbreviations: HSC, hematopoietic stem cells;BM, bone marrow;hMSC, human mesenchymal stem cells;CB, umbilical cord blood;FCS, fetal calf serum;TSLP, thymic stromal lymphopoietin;G-CSF, granulocyte colony stimulating factor;SCF, stem cell factor;FL, flt-3 ligand;GPA, glycophorin A; PC5, phycoerythrin 5-succinimidylester;NOG, NOD/SCID/common γ^{null}.

* Corresponding author. Tel.: +1 405 271 7905; fax: +1 405 271 8568.
E-mail address: kincade@omrf.ouhsc.edu (P.W. Kincade).

0022-1759/$ – see front matter © 2010 Elsevier B.V. All rights reserved.
doi:10.1016/j.jim.2010.06.002